Error-Encoded Vibrotactile Feedback to Enhance Motor Adaptation

BY

ALBERTO GNEMMI
B.S. Politecnico di Milano, Italy, 2009
M.S. Politecnico di Milano, Italy, 2012

THESIS

Submitted as partial fulfillment of the requirements
for the degree of Master of Science in Computer Science
in the Graduate College of the
University of Illinois at Chicago, 2012

Chicago, Illinois

Defense Committee:

Robert V. Kenyon, Chair and Advisor
James L. Patton
Pier Luca Lanzi, Politecnico di Milano

AKNOWLEDGEMENTS

Voglio ringraziare tutti coloro che, in momenti diversi e in vari modi, mi hanno aiutato in questa fantastica avventura che sono stati gli ultimi due anni. Innanzitutto voglio ringraziare la mia famiglia per avermi supportato e per avermi dato la possibilità di compiere questo ciclo di studi, per aver sempre avuto fiducia nelle mie capacità. Voglio ringraziare Robert V. Kenyon, il mio relatore a Chicago, per la fiducia che mi ha dato e per il costante aiuto dato in questa ricerca. Voglio ringraziare il prof. Andrea Bonarini per i preziosi consigli e per avermi aiutato con la pazza burocrazia del Politecnico. Meritano un ringraziamento particolare il prof. James Patton, Maura e Farnaz per l'aiuto nel fronteggiare un campo così nuovo ed intrigante. Infine ringrazio tutti gli amici che mi hanno seguito, da vicino e da lontano, durante l'intero corso di studi. Voglio ringraziare Leo, Gino, Samu, Marcy, Tia, la Raffa, Cri, Marghe e tutti gli altri amici che ho lasciato nel buon vecchio continente... Voglio scusarmi perchè è stato difficile mantenere i contatti, in particolare negli ultimi frenetici mesi in cui ho lavorato incessantemente alla tesi. Infine voglio ringraziare tutti gli amici, vecchi e nuovi, che hanno condiviso come questa avventura ammmmericana! Anto per la pazienza di avermi sopportato per ben due anni e per le fantastiche dosi di pizza che mi hanno dato la forza di andare avanti. Fra... forza campione! un giorno realizzarai il tuo sogno di lavorare al DEI! Fede per non avermi mai fatto sentire il bisogno di comprare un iPod. E ancora... Olga, Gio, Ju, Evgeniya, Lea. E infine voglio ringraziare il mio buddy Akki... nel bene e nel male non ti dimenticherò mai.

AG

TABLE OF CONTENTS

CHAPTER ***PAGE***

TABLE OF CONTENTS *(Continued)*

LIST OF FIGURES

LIST OF FIGURES *(Continued)*

LIST OF ABBREVIATIONS

CNS	Central Nervous System
EA	Error Augmentation
ET	Execution Time
IDM	Initial Direction of Movement
MPE	Maximum Perpendicular Error
nRnV	no Rotation and no Vibration catch-trial
RnV	Rotation and no Vibration catch-trial
RV	Rotation and Vibration trial
VRROOM	Virtual Reality and Robotic Optical Operations Machine

SUMMARY

The study of how humans learn a skilled movement and how they are able to compensate changes in the environment's dynamics is a topic of extreme interest, with a wide range of possible applications. Amplification of the error made while performing a task has been shown to be an effective technique to accelerate the learning process. The aim of this study is to present a preliminary investigation to understand if this technique works because it increases the subjects' awareness of error. Thanks to a modern Virtual Reality system, we studied if it is possible to enhance motor adaptation by providing to the subjects a vibrotactile feedback which is proportional only to the magnitude of the error. Our study asked 16 healthy subjects to perform a reach-and-stop task with their dominant hand, in a virtual reality environment where the visual field was rotated by 60 degrees. Our data shows that all the subjects were able to compensate the visual distortion, and to transfer what they learned to novel targets. The subjects who received the vibrotactile feedback were able to compensate the visual distortion almost twice as fast as the subjects of the control group. The results of this experiment suggest that a vibrotactile feedback has the potential to speed-up the adaptation. Further studies are necessary to better understand how to maximize the beneficial effect of vibration and to compare the effect of the vibrotactile feedback with the effect of other well known techniques used to enhance motor adaptation.

CHAPTER 1:

INTRODUCTION

Motor skills are an essential component of everyday life. All communications, from speech to body language and writing, are mediated via the motor system. This is the way organisms interact with the surrounding environment. The external environment, the organisms' body and the tasks performed are characterized, in realistic conditions, by dynamics which change over time. The control system has to be flexible enough to compensate for both sudden and unpredictable changes (e.g. a gust of wind) and long-term changes (e.g. the increase in dimensions of the body during puberty or the damages to the brain made by a stroke) [1,2,3].

The study of how humans learn a skilled movement and how they are able to adapt to changes in the environment's dynamics are a topic of extreme interest. A thorough knowledge of motor learning has a wide range of possible applications: for example athletes, surgeons and technicians that have to perform high precision tasks, casual sportsmen and artists that would like to learn a skill faster, pilots that have to learn a high risk task, and people with a movement disorder that have to relearn skills necessary for everyday life [4].

In the last decades, Virtual Reality and robotic devices are having a role of increasing importance in studies about motor learning. Such devices contain three characteristics which are particularly appealing for work in this area: reliable collection of data, easy reproducibility of the experiment and good control over subjects' sensory stimulation.

First of all, with these devices it is possible to collect data in an objective and reliable way. To have a good estimate of subjects' reaction time and performance it is necessary to collect data with a precision on the order of hundreds of a second. Modern electronic devices can guarantee such a performance. A second important characteristic is the capability of performing the same experiment with the exact same dynamic with different subjects. Robotic devices and virtual reality systems are able to reproduce exactly in the same way the complex effects which could be found in a motor adaptation experiment. Finally, the most important characteristic of virtual reality systems is the control on the subjects' sensory stimulations which they give to the scientists. All sensory perceptions can be properly generated by suitable devices with high precision and reliability.

Error Augmentation (EA) is an interesting technique used to enhance the motor adaptation in reaching tasks of the upper limbs [5]. A commonly accepted concept is that motor adaptation is a greedy optimization of the error made while performing a task and the effort expended in performing that task [6]. Error Augmentation exploits this concept: in some tasks it is possible to increase the performance of users by artificially increasing the error that they are making.

Error Augmentation experiments can be easily done with a Virtual Reality system. In [5], for example, the subjects have to reach some targets with their dominant hand, trying to make the reaching movements as straight as possible. The error produced by the subjects is continuously calculated, and it is increased by pushing the hand of the subjects with a robotic device (***Force EA***). Studies suggest that subjects are able to adapt faster when using this approach [7,8]. However, Error Augmentation is not limited to a physical augmentation of the error. In many studies [7,8,9,10], the error was only visually increased (***Visual EA***). In this way, the subjects only believed that they were making more error than what they were making in reality.

An aspect which these two Error Augmentation techniques have in common is that they increase the amount of error perceived by the subjects either physically or visually augmenting it. In this research we started investigating the hypothesis that Error Augmentation techniques work because they increase the awareness of error in the subjects. In other words, the subjects are more aware of the errors that they are making, and for this reason they tend to put more effort in reducing these errors. For this reason, in this research we provide the subjects vibrotactile feedback whose magnitude is encoded with the error that the subjects are making.

Such a vibrotactile feedback does not alter the task's dynamics and it is not experienced in everyday activities. For this reason, this feedback, if correctly interpreted by subjects, transmits only the information relative to the error made while performing the task. Vibrotactile feedback has been used to simulate contact forces in tele-operations [11,12], to help in navigation tasks [13,14] and to reduce spatial disorientation [15,16]. In [17] a vibrotactile feedback was successfully used to keep the elbow of some violin students in the right position inducing startle reactions. Before this research, this kind of feedback has never been used to accelerate a motor adaptation process.

To perform this experiment it was necessary to identify a motor adaptation task which could be used to evaluate the performance of the subjects. This task is a typical reach-and-stop task for the upper limbs; the subjects had to reach some targets with their dominant hand trying to make movements as straight and as quick as possible. The subjects had to compensate a 60 degrees rotation of the visual field which hampered the performance.

The protocol of the experiment was carefully designed to correctly evaluate the learning process of the subjects. In fact, the subjects could use different strategies to compensate the visual distortion. For example, a subject could learn the trajectory which his hand should follow to have an optimal performance. Alternatively, another subject could understand the nature of the distortion which is hampering the performance and then move his hand accordingly to improve his performance. These two strategies could have similar results, however it is easy to see that the second subjects was able to understand more deeply the dynamics of the distortion, and consequently he could be probably be able to transfer this knowledge in other similar situations. For this reason, it was important to not make any assumptions about how the subjects adapted. The protocol was designed in such a way to identify how deeply the subjects understood the nature of the perturbation.

The device used to perform the experiment was the Virtual Reality and Robotic Optical Operations Machine (VRROOM) of the Rehabilitation Institute of Chicago. This device is a complex Virtual Reality system that integrates a 3D virtual reality graphic display to provide visual immersion, a robotic arm to provide force feedback and a magnetic tracking system to trace the position of subjects' head and upper limbs. This device did not provide a vibrotactile display which fulfilled the requirements of this experiment. For this reason, it was necessary to modify the VRROOM and integrate a C-2 Tactor in the system, a lightweight and versatile vibrotactile display.

The code used to perform the experiment was written with the H3D framework. With this library it was possible to control both the graphics and the haptics of the experiment. The logic of the experiment was written in Python, while the graphical and haptic representation of the experiment was described with X3D. The applications used to perform the data analysis were written either in Python or in MATLAB.

This experiment showed that the subjects were able to understand the nature of the deformation. In both groups, the performance drastically improved since the moment in which the subjects were exposed for the first time to the visual rotation. Moreover, in both groups the understanding of the perturbation was deep enough to be generalized with new targets. The most important finding is that the vibrotactile feedback significantly enhanced motor adaptation to the 60 degrees rotation of the visual field. In fact, the subjects in the vibration group were able to compensate for the visual distortion almost twice as fast as the subjects in the control group.

The structure of this document is the following: Chapter 2 presents an introduction to motor learning, motor adaptation and a description of the state of art of the devices used study motor learning. Chapter 3 describes in details the devices used to perform the experiment, the protocol of the experiment and the techniques used to analyze the data. Chapter 4 presents the results of this experiment. In Chapter 5 the experiment's data is used to entail conclusions. Finally, Chapter 6 contains the conclusions of this work and the future developments.

CHAPTER 2:

BACKGROUND

The study of how humans learn a motor proficiency and how it is possible to speed up this process is a topic of extreme interest with a huge number of possible applications: ranging from athletes, surgeons and technicians that have to perform high precision tasks to casual sportsmen and artists that would like to learn a skill faster, from pilots that have to learn safely a high risk task to people with a movement disorder that have to relearn skills necessary for everyday life.

This Chapter presents human motor learning and describes how virtual reality systems can be applied to motor learning. At the moment a promising application is to enhance motor rehabilitation, and for this reason many examples refer to this field. However, it is important to consider that motor learning touches aspects of everyday life, and for this reason it is important to keep in mind the generality of its applications.

2.1 MOTOR LEARNING

While moving, a human subject interacts with a dynamic environment. Gravity, wind, objects, the ground, and the limbs themselves have dynamics that can be described using nonlinear models. This dynamic environment imposes, along with muscle forces, the trajectory of our limbs. The Central Nervous System (CNS) needs to deal with this dynamic environment to estimate the optimal movement pattern that should be used to reach a desired state, and to compensate for the forces which could be experienced in the upcoming movement.

Human ***motor learning*** is a complex process which is for the most part still unknown. It can be defined as a set of cognitive processes related to practice or experience that results in a relatively permanent and robust change in the capability to perform a skilled movement [3,18]. Alternatively, ***motor adaptation*** can be defined as the part of motor learning that deals with the changes of the environment dynamics.

Recently, robots were used to modify the environment dynamics and study the human's ability to deal with these changes. A usual experimental protocol to test motor adaptation in healthy subjects consists of a subject holding the handler of a robotic arm, while the robot alters the task dynamics by exercising some specific forces [4,5,19]. One of the most important conclusions of these studies is that, when the perturbation is suddenly removed (a so called ***catch-trial***), the subject moves his hand along trajectories which are turned in the opposite direction of the force. This phenomenon, called an ***after-effect***, persists for trials after the force field is removed. A possible explanation is that the subject is still predicting that the dynamics of the environment is altered by the perturbation force. This demonstrates that the CNS does not simply react to the external perturbation; instead, it tries to anticipate the expected dynamics and it makes its decisions based upon the past experience. These results allow to hypothesize that the CNS uses an ***internal model*** of environment's dynamics, and it constantly updates this model via the experienced errors [19].

The process of internal model formation can be properly described with a mathematical model. In this model, the sensory/motor system first estimates the error made while performing the current movement. Then, it changes the forces applied in the next movement proportionally to this error in the direction that should reduce the error [6,20]. In this mathematical representation the internal model is used by a *feedforward* component to inverse the environment's dynamics and to estimate the required muscle activation patterns. These studies suggest that the adaptation of this feedforward model plays a dominant role in the motor learning of subjects. However, this controller by itself is not able to compensate for the sudden and continuous changes of the environment dynamics. For this reason, it is hypothesized also the presence of a *feedback control system* which compensates the estimation error of the internal model and makes the whole system robust to environmental perturbations [19,21].

2.2 Virtual Reality, Robots and their Applications for Motor Learning

As described in the previous section, robotic devices have been used to investigate motor control. By using robots to apply novel forces to the limbs, investigators are exploring how the nervous system models the dynamics of the external environment.

Even if these devices have a fundamental role in research, their applications go beyond theoretical investigations and are actively used to enhance the learning process. In fact, recent studies suggest that robotic devices can be used to improve the motor learning process [4,5,7,22,23,24,25,26,27,28]. These devices enable high-intensity, repetitive, task-specific and interactive activities independent of instructor (or therapist) involvement [29]. The advantage of using a robotic device combined with a virtual reality environment is that such a device gives the scientist complete control over the ongoing task [4]. First of all, a virtual environment is able to gather at real time information about the performance of the subject. This gives the opportunity to the experimenter to have precise and reliable data about the experiment. Moreover, the system can, change the dynamics of the task accordingly to the subject performance, making it easier or more challenging. Another advantage is the reproducibility of the experiments. The computer system ensures that the task can be reproduced with the exact same conditions. Finally, a virtual reality system gives an almost complete control over the sensory stimuli presented to the subjects. The experimenter can both decide which feedbacks the subjects receive, and alter them at runtime.

The learning process of a subject using a virtual reality device is deeply influenced by his sensory experience that, as previously stated, can be controlled by the experimenter. It is important to distinguish between the *information* provided by a sensory feedback and the *sensory medium* used to provide this information.

Sensory mediums stimulate specific senses and, as consequence, specific areas of the brain. Moreover, they can actively influence the subject's state. An example of *active feedback* is a force that pushes the hand, while a sound emitted when the user is doing something wrong is a *passive feedback* that provides only information.

Three sensory mediums are commonly used in virtual reality systems:

1. **haptics:** this complex system uses sensory information derived from both receptors located into the skin (i.e. the *cutaneous* receptors) and receptors located in muscles, tendons and joints (i.e. the *kinesthetic* receptors). The haptic system can perceive a huge range of possible stimulations. However, the most used haptic stimulations in virtual reality are forces (active feedback), surface textures and vibrations (passive feedbacks) [30,31].
2. **hearing:** the auditory system is a passive feedback which can be used to give not only magnitude information, but also directional thanks to 3D surround systems.

3. **vision:** the visual system has been proved to be the predominant feedback in motor adaptation tasks of healthy subjects [32]. A possible explanation is that in everyday life visual information is the predominant kind of feedback that healthy subjects receive. However, it has been proved also that this feedback is not necessary for motor adaptation [33].

Each of these sensory mediums has been used with beneficial effects in motor learning experiments (vibration [11], force [5], hearing [34] and vision [7]).

Even if the *information* provided to the subject is independent from the sensory medium used, it is clear that some kind of information is better provided by specific feedback mediums. For example, a directional input is easier to provide with force feedback than with a vibration feedback, or a complex path is easier to be understood by a subject if provided with a visual feedback. An important point that must be kept in mind is that the information must be properly provided. Otherwise, the subject could have difficulties to understand its meaning, or even worse he could misunderstand it.

The following sections describe the two most commonly used robotic applications for motor learning: error reduction and error augmentation. Then, the state of the art is described for the devices that provide the two most frequently used feedbacks in motor adaptation literature: force and vision. Finally, the state of art of vibrotactile displays is described, because vibration is the sensory input used for the experiment described in this document.

2.2.1 Error reduction and error augmentation

Two methods used to study and/or enhance motor adaptation, which make use of robotic devices and virtual reality systems, are *error reduction* and *error augmentation*. The former summarizes all those techniques which help the users reducing the error that they are making and reducing the task's difficulty. The latter summarizes the approaches which hamper the user's performance, and make the task more difficult and challenging [4].

A typical error reduction task, called *guidance task*, consists in a preliminary phase in which the optimal way to perform the task is shown to the subject. This task tries to stimulate the mirror neuron system of the user, a neural network of the human Central Nervous System (CNS) which is active both when a person performs an action and when an action is being performed by others. This system is believed to be responsible of learning actions without performing them in the first person [35]. The task can be shown to the subjects through a visual representation (*visual guidance*), or can be passively felt by the users through a robot that moves their limbs (*robotic guidance*). Surprisingly, multiple studies suggest that there is no statistically significant advantage of using robotic guidance over a standard visual guidance [36,37,38,39]. However, there could be some positive benefit for some specific tasks [40].

Another typical error reduction task consists of using robotic guidance to reduce the difficulty of a task dynamics during the initial learning. In this way, the user needs to have an active role in the learning process, and the initial performance errors are reduced to make the task less dangerous or discouraging. The current goal of research is to identify the optimal amount of robotic assistance needed to make the task neither too difficult nor too easy [27,41].

The error augmentation techniques are diametrically opposite to the error reducing approach. As previously described, this technique increases the error made by the users to enhance the motor learning process. There are many possible reasons for which this approach may have a beneficial effect: the task may become more challenging, the users may be more aware of the errors that they are making, and they may be more prone to put more effort in performing the task. The error can be increased by physically moving the user's hand with a robotic arm (*force error augmentation*) [5,4,22], or the user can be tricked by making him believe that his performance is poorer than it really is (*visual error augmentation*) [7,8,9,10]. The studies done on error augmentation suggest that this is an effective way to speed-up the motor adaptation process [5].

2.2.2 Robotic devices

Robots used to provide force feedbacks in research and development projects can be divided into the following high-level groups: upper limbs robots, lower limbs robots, and robots devoted to cognitive/communication tasks. The following section describes more deeply the devices of the first group, because one of these devices is used in the experiment described in this document.

According to the classification made in [42], the robots used to alter the dynamics of upper and lower limbs can be subdivided into the following groups in terms of their mechanical design:

- **exoskeletons:** the human-machine interface extends all along the limb to which it is attached. These wearable devices are characterized by a number of degrees of freedom equal to the number of joints involved.

- **manipulandums:** the contact between the patient and the robot is only at the end of the robotic arm by means of an handler. The movements of the robotic arm are in the workspace of the hand, but they are not bounded to the joints of the user's arm.

Also, it is possible to subdivide these devices into two main categories if the control mechanism of these devices is taken in consideration:

- **impedance control:** in this control system, the robot device works as a force actuator, and this force is used to either hamper or assist the user's movement as a function of the movement kinematics. With this type of control, it is not necessary to specify the desired position or force. The user feels the intrinsic inertial and frictional forces, and in order to minimize this effect, the intrinsic mechanical impedance of the robotic arm must be small. There is only one loop in the impedance control system, and it is located between the human user and the robot. The robot measures the motion of the user and reacts with a force that is a function of the motion and of the impedance model. The overall loop is stable if the impedance controller is stable.

- **admittance control:** this control pattern is the inverse of impedance control. The robotic arm works as a generator of displacement, and the desired displacements is a function of the force measured by a sensor mounted in the handle. In this case, it is not necessary to have small intrinsic mechanical impedance. In this control system, there is one loop internal to the robot, which is not present in the impedance control. The robot measures the force applied by the user and reacts with a motion of the handle that is a function of this force. The motion is realized with a closed-loop controller, usually based on a PID model. The overall stability of the system does not depend only on the admittance controller, but also on the stability of the positional controller.

2.2.3 Virtual Reality Systems

Virtual Reality (VR) systems are frequently used in conjunction with robotic devices in motor learning studies and applications. Simple VR systems are two dimensional displays coupled with robotic instrumentation, in such a way to obtain a realistic interaction between the user and the virtual environment. More advanced systems give the users a full-immersion sensation in the virtual world thanks to three dimensional augmented reality graphic systems.

VR systems coupled with robotic devices have the huge advantage of giving a great control to the experimenter over the sensory stimulation of the user. In fact, this technology can generate a virtual environment such a way that the feedback intensity can be systematically manipulated to create the most optimal and individualized motor learning paradigm. For example, it is possible to exaggerate the movements of the user in order of amplifying their errors.

A huge advantage for research in motor adaptation and for therapeutic rehabilitation is the possibility of simplify the task's visual environment. In this way the subjects can focus on the task without being distracted by unnecessary objects, and the experimenter can remove from the environment elements which could unpredictably influence the experiment output. While very realistic and elaborated graphics are attractive to healthy subjects, they could be confusing for patients because the processing of complex information could be difficult if the users' CNS was affected by the impairment. Studies show that simple and schematic graphical environments could improve the performance of impaired subjects [43].

2.2.4 Vibrotactile Displays

In the past decades there has been a considerable interest in enriching the users' experience in virtual environments through the addition of haptic feedbacks. In the physical world, haptic stimulations are constantly present and extremely important to perform everyday activities, hence the use of such stimulations adds an interesting level of realism to a virtual reality experience. However, due to the technology gap that exists between visual and tactile displays, the latter are under used [30].

As previously described in this Chapter, the sense of touch is a complex system. Humans are able to perceive pain, temperature, chemical stimuli, state of limb joints, state of muscles, forces, texture of surfaces, and vibrations through many different kinds of receptors located inside the skin. There are six kinds of mechanoreceptors responsible of the detection of forces and vibrations. Each of them has peculiar mechanical and psychophysical properties, such as the frequency sensitivity, the threshold of two-point discrimination and the density in the skin.

The two main techniques to activate the skin mechanoreceptors are the electrical stimulation and mechanical stimulation. Other forms of tactile feedback such as air and liquid stimulation have been used but with a limited efficacy [30,12]. Mechanical stimulation is the technique typically used due to its safe and non-invasive nature. There are three main techniques of mechanical stimulation: vibrotactile stimulation, lateral deformation and normal deformation.

Vibrotactile displays stimulate the skin at frequencies in the 100-300 Hz range and typically transmit information about contact or texture. Vibrotactile displays are characterized by limited actuation power requirements and an easy control. Lateral deformation displays are associated with the simulation of friction. These devices usually utilize actuated mediums such as rotating drums to display lateral forces or the relative motion between the skin and the object. Both vibrotactile and lateral deformation displays are not able to transmit the perception of a surface shape, which can be provided by normal deformation displays. These displays typically use arrays of pins which are vertically actuated at low frequencies.

2.2.5 State of art of systems for motor learning applications

In this section it is briefly described the state of the art of robotic and virtual reality devices used in motor learning studies of the upper limbs.

2.2.5.1 University of Reading GENTLE/S

GENTLE/S is one of the largest European projects aimed to develop a therapeutic robotic arm [44,45,46]. This project, which was realized at the Tallaghn Hospital in Dublin (Ireland) and at the RBH-Battle Hospital in Reading (UK), brought to the development of a robotic system that uses a HapticMaster robotic arm. With this admittance controlled device the user can perform a robot-mediated motor tasks in a three dimensional virtual space, thanks to the coupling of the human arm movement with haptic interfaces and virtual reality technology.

Figure 1: HapticMaster admittance controlled robotic arm ant the GENTLE/S system.

2.2.5.2 Stanford Puma Robot MIME

The Mirror Image Movement Enhancer (MIME) is a six degrees of freedom robot manipulator based on the Puma 560 industrial robotic arm [47,48,49]. This device is able to apply forces to the paretic limb through a customized support of the user's forearm. The robot can move the user's forearm and has a wide workspace. Several modes of robot assistance are employed with MIME, such as passive, active-assisted, active-constrained, and bimanual modes. In the last case the device copies on one arm the mirrored movement of the other arm (typically the unimpaired limb of a hemi-paretic stroke survivor).

Figure 2: The Puma 560 robot of the MIME system.

2.2.5.3 MIT-MANUS

The MIT-MANUS project developed a two degree of freedom planar manipulator [50,51,52]. This device is well known because it was the first to be approved by FDA for clinical use. The robot is a low impedance system which guides people toward the correct motion. The clinical trial studies with MIT-MANUS first demonstrated a statistically significant improvement in the functions of the upper limbs as measured by the Fugl-Meyer scale, after only a four week treatment of daily sessions.

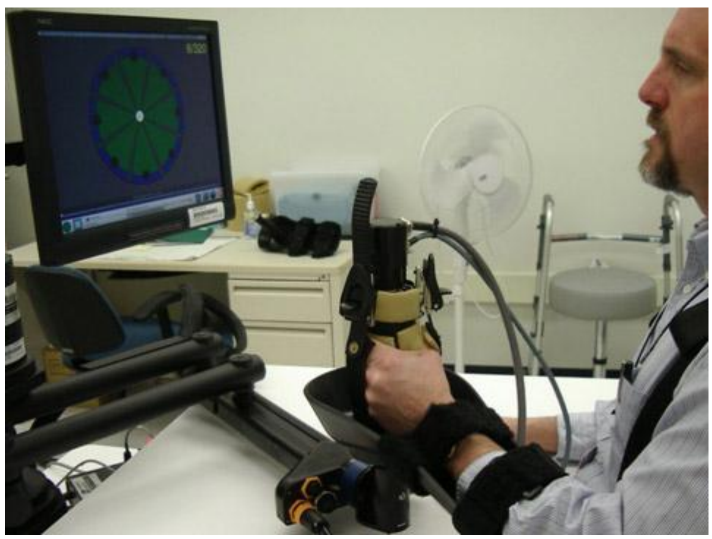

Figure 3: The MIT-MANUS.

2.2.5.4 RIC ARM Guide

The Assisted Rehabilitation and Measurement Guide (ARM Guide) was developed at the Rehabilitation Institute of Chicago [53,54,55,56]. This device has four degrees of freedom, and is used for reaching therapy with hemi-paretic stroke survivors. An actuator controls the position of the subject's upper limb, which is coupled to the device through a hand piece. This hand piece slides along a linear track in the reaching direction. The position of the arm is provided to the user through a real-time visual feedback.

Figure 4: The RIC ARM Guide.

2.2.5.5 T-WREX

The (T-WREX) was developed at the University of California-Irvine. This device is a five degree-of-freedom passive antigravity exoskeleton which is coupled with a computer workstation [57]. The exoskeleton relieves the weight of the upper limb with elastic bands attached to its frame. Movement and grip sensors allow the coupling between the passive device and the workstation. The aim of this project is the development of a device which gives the possibility to stroke survivors to practice reaching therapy with indirect supervision by therapists.

Figure 5: The T-WREX.

2.2.5.6 RIC-MANUS

The RIC-MANUS is a planar manipulator with two degrees of freedom developed at the Rehabilitation Institute of Chicago [58,59,60,61,62]. This device has a rigid parallelogram structure with direct drive of two brushless motors that provides a low intrinsic mechanical impedance. It has a planar workspace of 80×40 cm and it uses optical encoders to measure hand movements with high resolution (0.1 mm). This device can generate forces from fractions of 1 N up to 50 N. A projector displays a two dimensional representation of a graphic environment on a surface which can completely occlude the workspace. The graphic environment is coupled with the robotic device to ensure real-time interactivity.

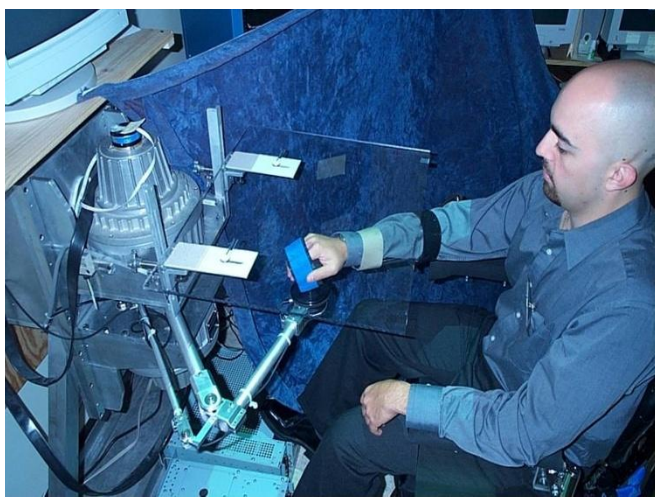

Figure 6: The RIC-MANUS.

2.2.5.7 RIC VRROOM

The Virtual Reality and Robotic Optical Operations Machine (VRROOM) is a complex virtual reality system which integrates a PARIS 3D virtual reality graphic display to provide visual immersion, a PHANTOM Premium 3.0 robotic arm to provide force feedback and a Flock of Birds magnetic tracking system to trace the position of subjects' head and upper limbs [63,64]. This device, provides a three dimensional workspace of 90 x 90 x 30 cm, and the robotic arm is capable of exercise forces along three degrees of freedom and up to 22 N of intensity. The tracking system and the augmented reality visual display permit a perfect coupling between the virtual and the real environment, providing an interesting level of immersion to the user. This device is better described in Section 3.1.

CHAPTER 3:

MATERIALS AND METHODS

This Chapter provides a complete description of the Materials and of the Methods used to perform the experiment illustrated in this document. In Section 3.1 it is described the Virtual Reality system used in the experiment, the Virtual Reality and Robotic Optical Operations Machine (VRROOM) situated at the Rehabilitation Institute of Chicago. This apparatus includes a 3D graphic system, a robotic arm and a vibrotactile actuator which was installed specifically for this experiment. The experimental protocol is described in Section 3.2 and finally, in Section 3.3, the techniques used to analyze the data are explained in detail.

3.1 EXPERIMENTAL APPARATUS

The apparatus used in this experiment is the Virtual Reality and Robotic Optical Operations Machine (VRROOM) depicted in Figure 7. This device is a complex Virtual Reality system that integrates a 3D virtual reality graphic display to provide visual immersion, a robotic arm to provide force feedback and a magnetic tracking system to trace the position of subjects' head and upper limbs. This device, in its original configuration, cannot provide the vibrotactile feedback required by the experiment. For this reason, it was necessary to modify the original version of the VRROOM device and add a vibrotactile actuator.

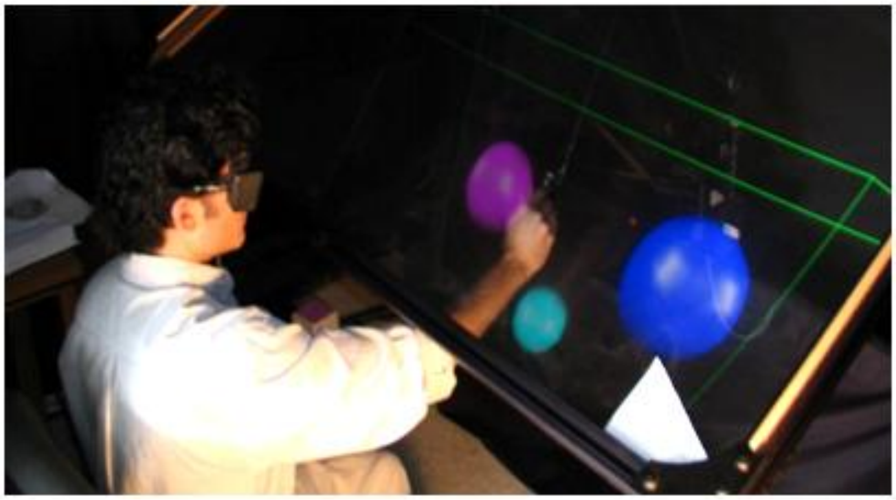

Figure 7: *Components of the VRROOM apparatus. An experimental subject is seated at the apparatus and he is interacting with the 3D environment. The robotic arm is providing the haptic feedback and the PARIS display is graphically visualizing some large spheres. Not clearly visible are the magnetic tracking sensors that are placed on the head and limbs of the subject to detect the position of eyes and upper limbs in space.*

The VRROOM was chosen to be used in this experiment because it fulfills the requirements that were determined during a preliminary analysis. These requirements do not take into consideration only the immediate requirements of the experiment, but also the possible requirements of follow-up experiments. These requirements [63,64] can be summarized as follows:

1) **Data collection:** it is necessary to collect at run-time the movements of subjects' upper limbs and the sensory stimulations supplied to subjects. The system has to change if necessary the experiment's behavior based upon the performance of each subject;

2) **Wide range of movements:** the system must provide a wide workspace and sufficient degrees of freedom to allow the complex behaviors seen in everyday tasks. A subject,

while seated, must be able to completely extend the upper limbs in the hemispheric space in front of him;

3) **Superimposition of virtual objects onto the real world:** the coordinate system of the graphic representation must be aligned with the coordinate system of the haptic device to maintain a coinciding model. For example, the virtual representation of the user's hand must occupy the same position of the real hand that the user is utilizing to interact with the Virtual Reality environment. Once aligned, the union of graphics and haptic representations presents an immersive illusion to the user. In the standard computer/mouse paradigm there is no superimposition: the cursor on the screen is the virtual representation of the user's hand, but it is not superimposed onto the hand of the user. The reason to have a superimposition is to avoid a mental coordinate remapping between the real world and the virtual world;

4) **Multiple feedbacks:** experiments of motor learning usually involve different kinds of sensory stimulations. For this reason, is important to have the control over multiple sensory stimulations: sight, hearing and haptic. Moreover, the system must be built in such a way to avoid stimuli from the external environment;

5) **High quality graphic display:** a display with low resolution and high latencies can hamper performance even in healthy subjects [65,66,67,68]. For this reason, it is important to use a visual display that will allow users to achieve their peak performance levels.

The VRROOM meets these requirements, and does not require an extensive work of building and calibration because it is already operational at the Rehabilitation Institute of Chicago. This device was built to perform motor learning and motor recovery studies on both healthy and impaired subjects. For this reason, it has been tested multiple times and it proved to be a reliable and versatile device [63,64,69,70,71].

3.1.1 Personal Augmented Reality Immersive System (PARIS)

The Personal Augmented Reality Immersive System (PARIS) is the visual display system used by the VRROOM, and it is depicted in Figure 8. This device was developed at the Electronic Visualization Lab (EVL) at the University of Illinois at Chicago. It is the result of the lessons learned by EVL's engineers while developing the PARIS' predecessors: the CAVE [72] and the ImmersaDesk [73].

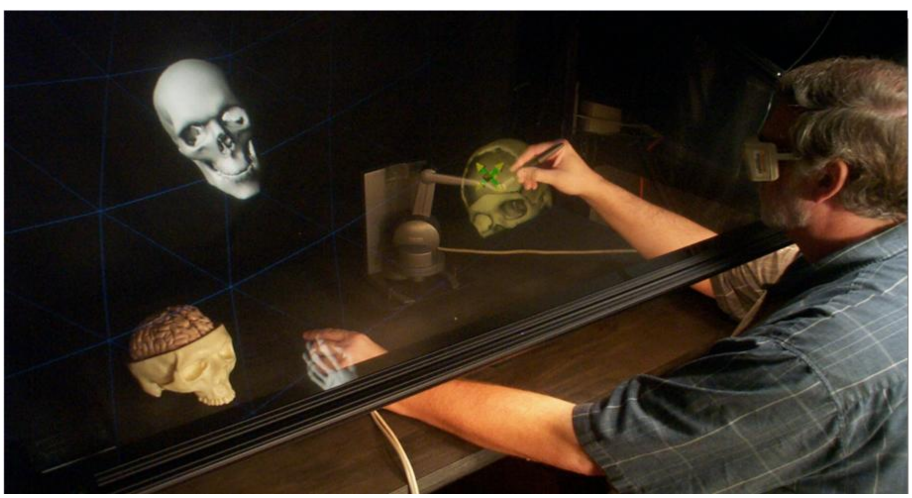

Figure 8: The PARIS system. The user is utilizing an application to design pre-surgical cranial implants. Similarly to the VRROOM, the experience of the user is augmented with tactile sensations provided by a haptic device. However, the workspace is compact and restricted to a sphere with a diameter of about 20 cm.

PARIS is the highest quality see-through augmented reality system available [63,64,74,75]. A description of how PARIS works is given in Figure 9. This device projects stereographic images onto a half-silvered mirror, allowing users to view virtual objects superimposed onto the real world. Adjusting the lighting levels under the half-silvered mirror allows subjects to view their own limb and only the artificial virtual elements that are needed.

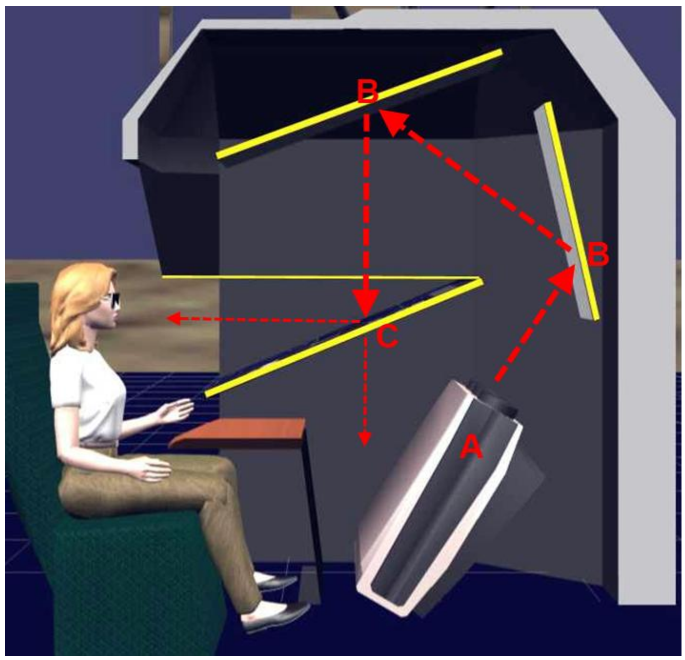

Figure 9: A rendering of the PARIS. The 3D images projected by the digital projector (A) are reflected by two mirrors (B), then are semi-reflected by a half-silvered mirror (C), and finally they reach the user. A system of magnetic trackers is used to identify the position or the user's head, and update accordingly the images.

Two important depth perception cues, *occlusion* and *accommodation*, are supported by PARIS [74,75]. In a conventional projection-based virtual reality display, an object in front of the hand is obstructed by the hand itself. This *occlusion* causes a visual conflict because the hand, which should be behind the object, appears in front of the object. The half-silvered mirror in the PARIS display superimposes the displayed image over the hands. The second depth cue, *accommodation*, refers to the process by which the muscles controlling the shape of the crystalline lens inside the eye adjust its optical power to maintain the focus on an object as its distance from the viewer changes. In a conventional VR display the eye will always be focus on the display screen. However, with a stereo image, the user's eyes converge to look at the 3D point where the virtual object is located. If the virtual object is not located on the screen, these two cues create a conflict. In the PARIS, the virtual display is located in such a way that the hands and the virtual object are at the same distance.

A cinema-quality digital projector (Christie Mirage 3000 DLP) displays the 1280x1024 pixel image over a five foot wide half-silvered mirror resulting in a 110° viewing angle. Infra-red emitters synchronize the display of separate left and right eye images through LCD shutter glasses.

An Ascension Flock of Birds magnetic elements track movement of upper limbs and head so that the visual environment is rendered with the appropriate perspective. Multiple tests have shown that neither the aluminum parts of the PARIS system nor the electromagnetic radiation from the motors of the robotic devices distort the readings of the magnetic tracking system.

3.1.2 PHANTOM Premium 3.0

In Figure 10 it is depicted the PHANTOM Premium 3.0 by SensAble Technologies, a robotic arm located below the half-silvered mirror of the PARIS device. This device is used to provide a haptic feedback to increase the realism of users' interaction. The PHANTOM Premium 3.0

provides six degrees of freedom of positional sensing (x, y, x, pitch, roll and yaw) and three degrees of freedom of force feedback (x, y, z).

Figure 10: A Phantom Premium 3.0 and its encoder. The encoder is connected with the VRROOM workstation via a parallel port (EPP) interface, and transmits information back to the external computer with a frequency of 120 Hz. The range of movement of this robotic device is equivalent to a full arm movement pivoting at shoulder.

This device provides a workspace measuring up to 900 x 900 x 300 mm and is capable of generating a maximum continuous force of 3 Newton (N) with transient peaks of 22 N. The encoder of this device runs asynchronously with a computer for stable and uninterrupted control. Two other robotic arms are present in the VRROOM and can be substituted to the PHANTOM if needed: the WAM (Barrett Technologies) for strong impedance control applications that require precisely controlled forces ad torques and a HapticMaster (FCS technologies) for strong admittance applications that require precisely controlled motions.

3.1.3 C-2 Tactor

The VRROOM, in its original configuration, cannot provide the vibrotactile feedback required by the experiment described in this document. The workstation that controls the PHANTOM Premium 3.0 sends inputs to change the haptic feedback with a maximum frequency of 120 Hz. In previous experiments, a fast series of forces applied in opposite directions was used to simulate a vibrotactile feedback. However, with this technique it is not possible to control precisely the amplitude and frequency of the vibration. Moreover, sending commands to the robot with a frequency of 120 Hz impose an upper bound to the vibration frequency that is far below the frequency of 250 Hz required for an ideal stimulation of skin's mechanoreceptors [12,30,31,76]. For this reason, it was necessary to modify the original version of the VRROOM apparatus, and add a vibrotactile actuator.

This vibrotactile device, the C-2 Tactor (Engineering Acoustic, Inc.), is controlled by a mono-channel audio signal emitted by the VRROOM's workstation. This audio signal must be correctly amplified to obtain the desired vibration displacement.

3.1.3.1 The actuator

The C-2 Tactor is a linear actuator that has been optimized to create a strong, localized sensation against the skin (Figure 11a). This vibrotactile actuator is a voice coil transducer, as it is illustrated in Figure 11b. In this type of device a moving contactor is located outside the housing and is lightly preloaded against the skin. The C-2 Tactor works with a principle similar to the one used for audio speakers: the coil is located in a magnetic field and, when an electrical signal is applied, the coil is pushed along its axis with a strength proportional to the current applied. The contactor oscillates perpendicular to the skin, while the surrounding skin area is shielded with a passive housing [77].

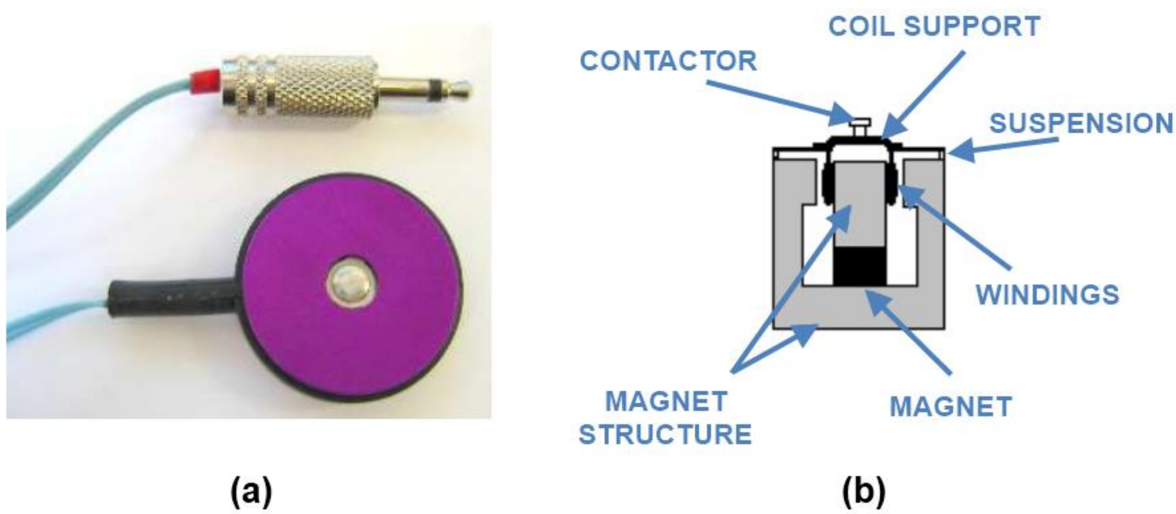

Figure 11: A C-2 Tactor. Image (a) shows the actuator and the 3.5 mm jack used to connect this device to the VRROOM workstation. Image (b) shows a scheme with the components of a voice coil transducer (image adapted from **[78]**).

The C-2 is designed with a primary resonance in the 200-300 Hz range (Figure 12), to have optimal vibrotactile efficiency. In fact, this resonance frequency coincides with the peak sensitivity of Pacinian corpuscles, the skin's mechanoreceptors that are believed to perceive vibration [12,30,31,79]. The C-2 Tactor's high force and displacement levels allow the vibration to be easily felt in many different locations on the body, even through multiple layers of clothing.

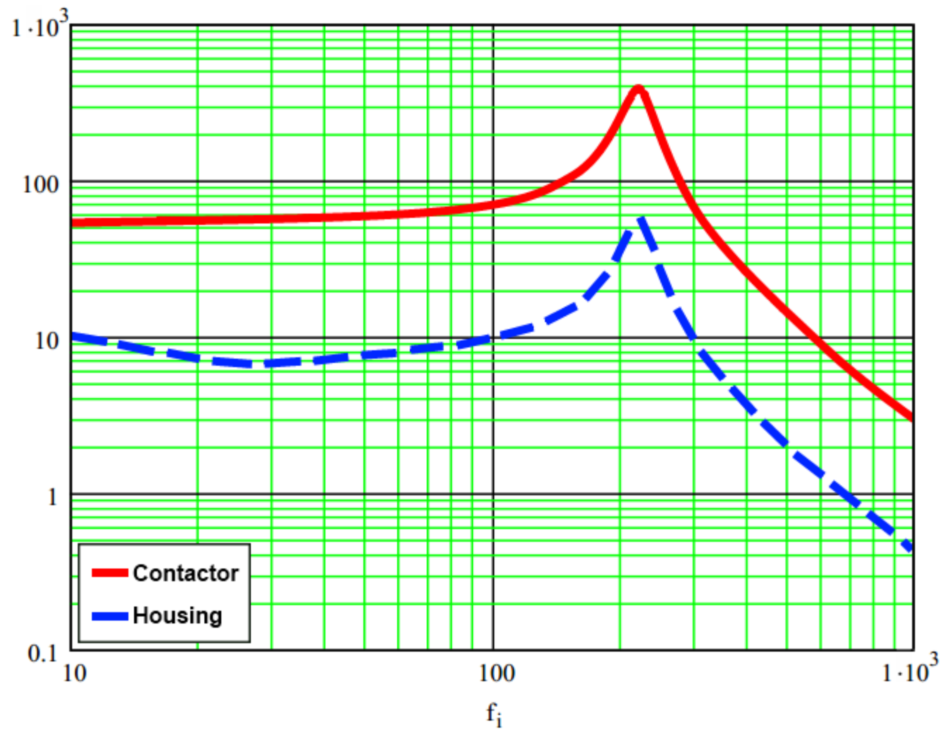

Figure 12: Peak-to-peak displacement level in μm of a C2 Tactor preloaded onto the skin with a constant drive of 300 mA. The red curve is the displacement of the contactor, while the blue curve is the displacement of the actuator's housing. The resonance peak of this device is between 200 and 300 Hz. (Image adapted from **[80]**)

The C-2 Tactor is an extremely lightweight and portable actuator, thanks to a diameter of 3 cm and a weight of 17 grams. These properties grant to this device the possibility to be placed on the fingertips of a subject without hamper performance.

This actuator has a nominal impedance of 7 ohms and should be driven using sine wave bursts with a frequency of 250 Hz and a current of 25mA RMS nominal. However, it can sustain bursts with a current of 50mA RMS nominal for short durations. The audio card of VRROOM's workstation does not provide an audio output strong enough to drive this device. Hence, it was necessary to build a high power signal amplifier to increase the signal strength.

3.1.3.2 The Signal Amplifier

The audio output of the VRROOM's workstation was not strong enough to pilot the C-2 Tactor. This signal with the maximum power was 659.3 mV RMS (Figure 13a), a value extremely lower than the 3700 mV RMS required to drive the C-2 Tactor with the maximum power (Figure 13b). For this reason, a high-power signal amplifier was built to increase the signal.

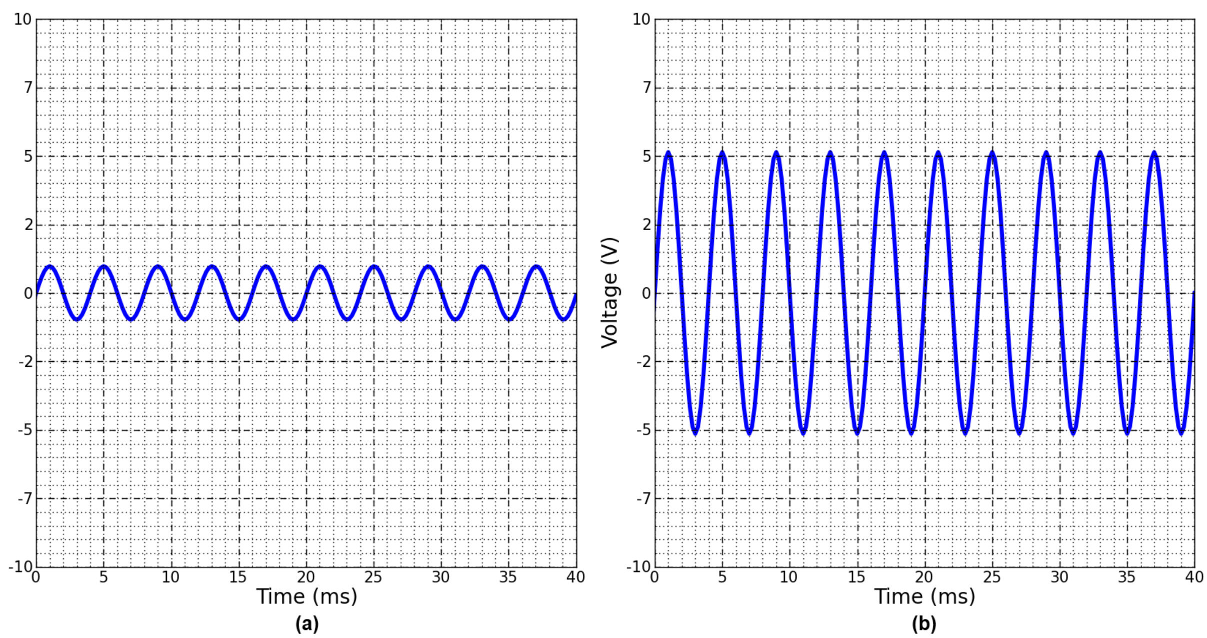

Figure 13: The effect of the signal amplifier built to control the C-2 Tactor. Figure (a) shows the voltage of the input audio signal, while figure (b) shows the voltage of the output audio signal.

The circuit used to amplify the signal is a standard inverting amplifier (Figure 14). To fulfill the voltage and current requirements of the C-2 Tactor, the operational amplifier used is the

OPA547 of Texas Industries. This low-cost, high-voltage/high-current operational amplifier has a maximum continuous current output equal to 750 mA. We have:

$$G = -\frac{R_f}{R_{in}} = -5{,}6 \text{ , and } V_{out} = G * V_{in} = -5{,}6 * V_{in}$$

Given a maximum input of 659.3 mV RMS, the maximum output is about 3700 mV RMS. The max current measured in the C-2 Tactor was equal to 0.35 A RMS. Such a value was chosen because it is halfway between the standard driving current of 0.25 A RMS and the suggested limit value of 0.5 A RMS.

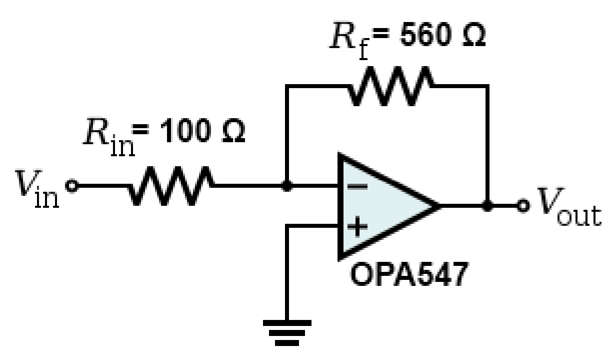

Figure 14: The circuit schematic of the inverting amplifier.

3.1.4 H3DAPI Framework

The experiment code was written with the H3DAPI framework. H3DAPI is an open source development framework which uses OpenGL and X3D to control both graphics and haptics. This framework is independent from both the development platform and the haptic device used. These factors, and the fact that it supports stereographic displays, made this framework an ideal choice for the development of this experiment's application.

The H3D framework is written in C++ and it uses OpenGL for graphic rendering and HAPI for haptics rendering. The front-end application is written in Python and X3D. Python is used to write the logic of the application, while X3D (which uses the XML syntax) handles the model of the world. The virtual world, including both graphic and haptic objects, is defined in X3D through a scene graph.

3.2 EXPERIMENT PROTOCOL

The experiment described in this document used a vibrotactile feedback proportional to the error done in a reach-and-stop task for the upper limbs. The subjects were asked to compensate a 60 degrees rotation of the visual field, which is a novel visuo-motor perturbation. This experiment was used to investigate if a system that increases the error awareness can enhance motor adaptation in healthy subjects.

3.2.1 Rationale

As it is described in Chapter 2, a recent study [6] suggests that motor adaptation is nothing else than a greedy optimization between the errors occurred while performing a task and the effort required to perform it (Figure 15). According to this hypothesis, people try to find the right balance between error and effort, and the weights associated to these variables are subjectively decided. The basic idea underlying Error Augmentation is that the weight associated to the error is artificially increased to increase the effort of the subject in performing the task.

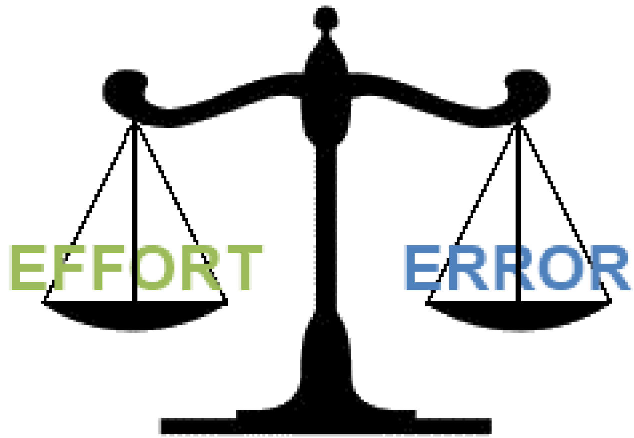

Figure 15: Motor Adaptation is a greedy optimization of error and effort.

Many studies [4,7,8,10,69,81] suggest that Error Augmentation can successfully enhance motor learning. But how can Error Augmentation (EA) be defined? In Section 2.2 two kinds of Error Augmentation are described: Force EA [5,7,8,22] and Visual EA [7,8,9,10,69]. *Force EA* actively worsens the performance of the subject; it amplifies the errors that the subject would normally make and it modifies the task to be more challenging. On the opposite side, *Visual EA* deceives the subject making him believe that his performance is worse than what it is in reality. It is possible to assume that a “black box” exists in our mind which takes as input all our sensory perceptions and our experience, and calculates a subjective representation of the error made while performing a task. Hence, it is possible to define Error Augmentation as a technique that alters a subject’s sensory perception to artificially increase his subjective perception of error (Figure 16).

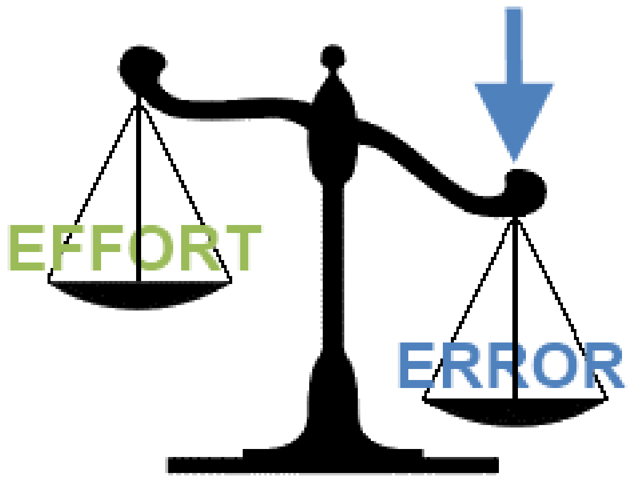

Figure 16: Error Augmentation alters a subject's sensory perception to artificially increase his subjective perception of error.

The basic idea of the experiment described in this document can be described as follows. Let's take, as example, a person who is speaking a language he is not proficient in. While this person is speaking, he is able to evaluate his speech performance. However, he is not likely able to notice all the errors he is committing. This person will be aware of more errors if he is using an ideal device that alerts him every time he makes a mistake. The direct consequence is that, most likely, the person will evaluate his performance being poorer than without this feedback. Is the increase of error awareness a kind of Error Augmentation? In fact, the device of the example is increasing the subjective perception of error. It is difficult to say in the specific case of the speaker, because there are complex psychological implications. However, it is a reasonable hypothesis in the case of quick reaching movements with the upper limbs.

The experiment described in this document tries to clarify if it is possible to enhance learning by increasing the subjects' awareness of their error. To accomplish this goal, the protocol applied is similar to the one used to show the advantages of Error Augmentation in reaching tasks. Typically, in an Error Augmentation experiment the error is actively increased with Force EA or forged with Visual EA. Instead, in this experiment, a vibrotactile feedback emphasizes the subjects' errors.

A vibrotactile feedback is suitable for this task because, if used properly, is capable of successfully transmit information without hampering performance [11,23,79,82,83]. For example, in [11] not only a buzzer was successfully used to substitute the force feedback in a tele-operated task, but it also led to better performances than the use of a standard force feedback. The experiment performed by Massimino is particularly interesting because it shows that it is possible to successfully substitute the effect of a force feedback with a vibrotactile feedback. For this reason we hypothesized that it is possible to successfully apply the protocol used for an Error Augmentation reach-and-stop task, and substitute the force feedback with a vibrotactile feedback. The advantages of using a vibrotactile feedback are multiple. First of all, the use of vibration does not have the risk of instability that the force feedback has. For this reason it is possible to increase at will the gain used to provide the error feedback [11]. Moreover, the perception of vibration is typically underused in reaching tasks [30]. Hence, it is reasonable to hypothesize that the amount of information sent to the brain can be increased using this channel. Finally, studies suggest that vibrotactile perception can be elaborated quicker [11,84] and with less cognitive workload [82] than other sensory perceptions, such as force perception or vision.

The main challenges approached to accomplish this experiment were two: finding a way to make a reaching task novel to healthy subjects and finding a way to evaluate the learning process of the subjects.

A 60 degrees rotation of the visual field with respect to the center of the workspace was applied to make the task novel. This visual deformation was chosen because it was previously used in multiple studies about dynamic adaptation [7,8,9,10,69], and these studies suggest that healthy subjects can adapt to this deformation after some hundreds of repetitions.

Learning is a difficult parameter to evaluate because it cannot be directly measured; it is only possible to measure the consequences of learning. When a disturbance is introduced in a task, such as a visual distortion, a subject can use different strategies to compensate the perturbation, and increase his performance. For example, a subject could learn the trajectory which his hand should follow to have an optimal performance. Alternatively, another subject could understand the nature of the distortion which is hampering the performance and then move his hand accordingly to improve his performance. These two strategies could have similar results, however it is easy to see that the second subject was able to understand more deeply the nature of the distortion, and consequently he could be able to transfer this knowledge to other similar situations. For this reason, it is important to not take any assumption about how the subjects adapted. A deeper understanding of the environment dynamics corresponds to the creation of a good <u>***internal model***</u> of this dynamics. This internal model of the perturbation is used to predict the muscular activation pattern that should be used do reach a given location in space [4,20,81,85]. For this reason, it is not enough to measure how the error decreases while the task is repeated over time in the attempt to infer the presence of learning. A way to infer learning is to analyze what happens if suddenly the perturbation is removed. For example, in [5] the subjects have to reach a target with a force pushing their arm. If a subject is compensating the force only by increasing the stiffness of his arm (feedback control), then when the force is removed the error disappears instantaneously. On the other hand, if the subject learns how the force is applied and he uses this knowledge to push against this force, then when the force is removed the prediction is wrong and he will make errors until he will correct the prediction. For this reason, it is necessary to introduce in the experiment some "catch-trials" where the visual deformation is removed, and these catch-trials are used to show the presence of learning.

3.2.2 Subjects

A total of sixteen healthy subjects participated in this study, and all of them signed a consent form that conformed to federal and University guidelines as approved by the Institutional Review Boards of both University of Illinois at Chicago and Northwestern University. Their ages ranged between 19 and 35 years, and seven of them were females. All the subjects had a normal or corrected-to-normal vision, and no history of significant neurological or orthopedic disorders. Each subject used his dominant hand; two subjects were left handed.

Two subjects were not naïve to motor adaptation experiments, but no one had previously done experiments that require adaptation to a rotation of the visual field. The subjects were randomly and evenly divided into two groups. Each subject participated only in one experiment to prevent crossover effects.

3.2.3 Task

A standard reach-and-stop experiment with adaptation to a rotation of the visual field [7,8,9,10,69] was done on healthy subjects using the equipment described in the previous sections.

The subjects sat in the VRROOM in front of the PARIS. They held the handle of the PHANTOM Premium 3.0 with their dominant hand, and a C-2 Tactor was attached firmly to the index fingertip of this hand. The C-2 Tactor was attached not only to the subjects of the vibration group, but also to the subjects of the control group. A small green sphere with a radius of 1 cm indicated the position of the subject's hand, while the real hand was hidden behind a black curtain and not visible to the subject. The subjects were instructed to reach targets that appeared on the screen with a movement as quick and straight as possible, and then return to the start position. Three ***targets*** appeared on the screen in a random order. This order was random within a session, but unvaried between different subjects. The three targets were equidistant on a 10 cm radius circumference, while the start position was located at the center of the circle (Figure 17a). The three targets and the start position were represented by a light blue sphere with a radius of 2 cm. The circle was located on a plane tilted 30 degrees with respect to the plane orthogonal to the subject's chest (Figure 17b). The rotation of the plane and the position of the circle on the plane were chosen in such a way to make the reaching movements comfortable to subjects with a short range of reaching.

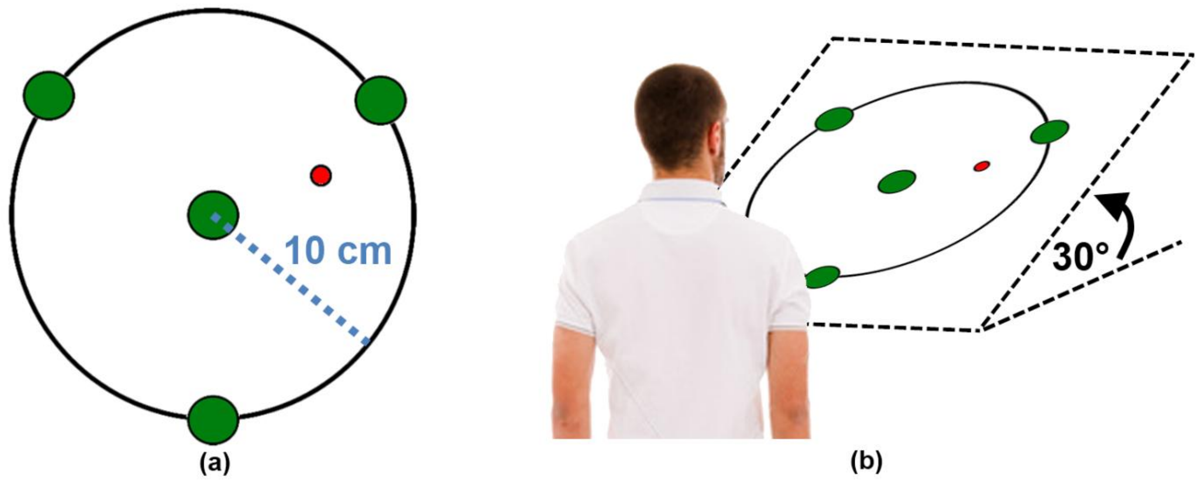

Figure 17: The position of the targets in the workspace; during the experiment, the targets are represented by green spheres, and the cursor is represented by a red sphere. Figure (a) shows that the three external targets are equidistant on a 10 cm radius circumference. The first external target was correspondent to a 30° angle, and the others targets are 120° apart from each others. Figure (b) shows that the circle is on a plane tilted by 30°. This inclination granted comfortable reaching movements.

The movements of the hand were constrained to the plane where the targets were lying to reduce the influence of errors caused by a lack of depth cues. An example of the effect that this lack of cues can have is shown in Figure 18. This image depicts typical trajectories of a subject who had to reach four targets in a virtual environment with weak depth cues; it is possible to entail from these trajectories that the subject had problems to identify the exact position of the targets. In fact, the trajectories are split into two movements: a first quick movement to reach the position where the subject believed that target was, followed by a second movement to reach the real position of the target. For this reason, the experiment can be considered as a two dimensional reach-and-stop experiment in a three dimensional workspace.

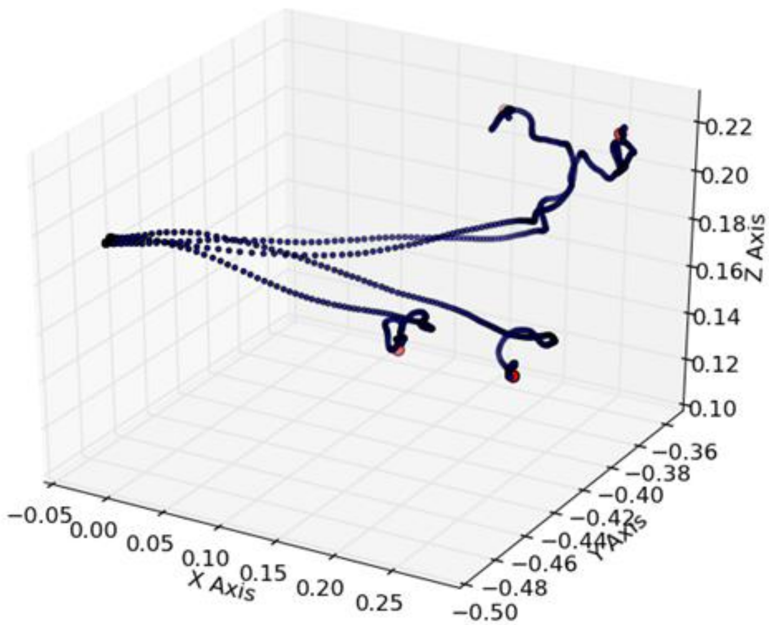

Figure 18: A pilot study to analyze the effect of movements in a 3D environment with few depth cues. The subjects had to reach four targets (red dots) that were shown in a random order. No visual distortions were applied. Analyzing the trajectories of the subjects it is evident that the subjects had problems to calculate the real position of the targets. The trajectories were split into two movements: a first quick movement to reach the position where the subject believed that target was, followed by a second movement to reach the real position of the target.

A ***trial*** was defined as a reaching movement from one target to another. Each subject, every time that a target was displayed, had to reach the new target as soon as possible and to stay in that position until the next target was displayed. Trials where the hand starts moving before the target is displayed were discarded, and a new trial was started. The targets were shown in a random order to avoid predicting the location of subsequent targets. Each movement from the central target to a target on the circumference is called ***outward movement***, is followed by an ***inward movement*** that takes the hand back to the central position. Only the outward movements were considered for this experiment, because the inward movements were more prone to automatic movements. To successfully reach a target the cursor had to stay for at least 200 milliseconds inside the radius of the target.

The target changed its color to red if the subject took more than 0.7 seconds to reach it to signal a particularly slow movement [85]. The subjects were instructed to reach the target as soon as possible. This quick movement requirement was used to minimize subjects' intra-trials learning. In fact, the slower the movement the easier it is to reach the target thus reducing drastically the error done.

A reach-and-stop task without perturbation is a trivial task for healthy subjects. Hence, learning is minimal or absent in such a task. For this reason, a 60 degrees counterclockwise rotation of the visual field centered on the central target was applied on the cursor to make the task novel (Figure 19). However, the unperturbed task was still used at the beginning and at the end of the experiment to compare the performance of the unperturbed task with the perturbed one. The rotation of the visual field is applied only to the cursor, and not to the targets. Consequently, subjects could understand that the visual distortion was present only by moving their hand.

Figure 19 shows what happened to the cursor and the subject's hand in the first movement of the learning phase. This figure shows the subject moving his hand from the central target, where the hand was, to the only visible target. Because the subject is not aware of the visual distortion, his central nervous system (CNS) applies the standard strategy to reach the target, and the subject moves his hand directly towards the green target. However, the position of the red cursor is rotated by 60 deegrees counterclockwise, therefore the cursor does not move towards the target. To reach the target, the subject must move his hand along a trajectory that is rotated 60° clockwise.

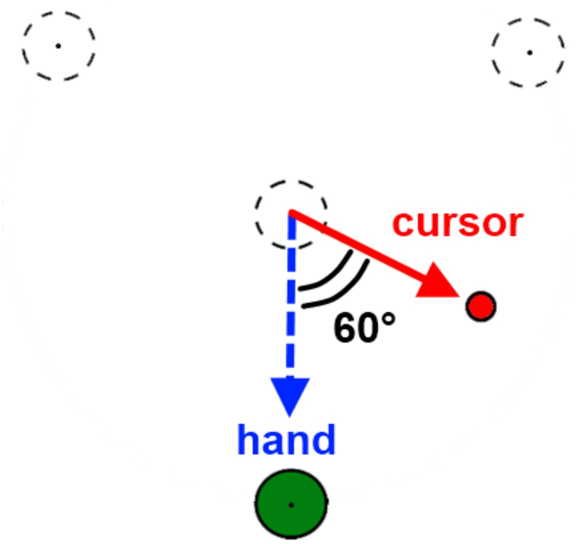

Figure 19: Effect of the visual rotation. In the early trials of the learning phase, when a subject tries to reach the only visible target (green), he moves his hand (blue) directly towards the target. However, the cursor (red) moves along a completely different trajectory due the visual counterclockwise rotation of 60°.

The subjects are equally distributed into two groups: vibration group and control group. The difference between these two groups is that a vibrotactile feedback proportional to the error is provided to the vibration group by the C-2 Tactor. The error is defined as the vector that connects the position of the cursor to its orthogonal projection on the ideal line which connects the starting target with the target that the subject is trying to reach (see Section 3.3.2.1: Maximum perpendicular distance). The vibration is a value proportional to the magnitude of the vector $error$, and it is defined as:

$$vibration = \begin{cases} \dfrac{\|error\|}{MAX\_ERROR}, & if\ \|error\| < MAX\_ERROR \\ 1, & otherwise \end{cases}$$

with $MAX\_ERROR = 3\,\text{cm}$. Hence, the vibration is a value between 0 and 1, with 0 corresponding to no vibration and 1 corresponding to the maximum possible amplitude of vibration. The maximum value of vibration is reached when the error is greater than 3 cm. Figure 20 shows the result of a pilot test done to choose the saturation value of the vibration. This value is chosen so that saturation would occur only in the early learning phase where larger errors were made, but also so that the vibration was not too small in the late learning phase.

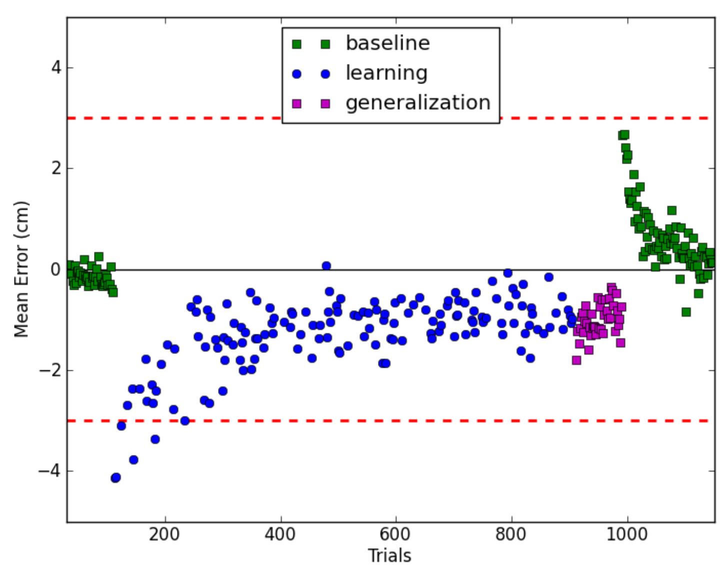

Figure 20: A pilot study performed to identify an optimal saturation value for the vibration. The dots represent the average error during a trial, and the red dotted lines represent the saturation value equivalent to an error magnitude of 3 cm. The saturation value should guarantee saturation only in the very early learning phase, and should avoid having a too small vibration in the late learning phase.

The experiment was divided in ***blocks*** of usually eighty movements, and the time required to finish a block of movements varied from 2 to 5 minutes. To avoid fatigue, subjects were obliged to *rest* after finishing each block. There were twelve rests of 40 seconds, and two rests that were 120 seconds long. The subjects were not allowed to skip the rests, and during the two long rests they were allowed to stand up and move around the experiment room.

The experiment can be subdivided into five phases:

1. **Familiarization:** in this phase the subject gets familiar with the characteristics of the devices used for this experiment and with the unperturbed reach-and-stop task. This phase was necessary because the goal of the experiment was to observe how subjects adapt to the visual distortion, and the lack of familiarity could introduce some noise in the first measurements. At the beginning of this phase, the subject was exposed to the whole range of possible vibrations, and the experimenter checked if the subject was annoyed by this stimulus. The vibration was not above the pain threshold for none of the subjects. After the familiarization with the vibrotactile device, the subject had to perform 60 trials of the reaching task (30 outward and 30 inward) with no vibration and no visual rotation. During these movements the subject had to become familiar with the workspace, the graphic elements and the task.

2. **Baseline:** this phase is used to evaluate the baseline of the unperturbed reach-and-stop task. During the 80 trials of this phase (40 outward and 40 inward), neither the vibration nor the visual distortion is present. The features extracted from this phase are particularly interesting because they can provide precious information about how the

subjects perform when the distortion is not present. The error in this phase is expected to have a small variance and to be close to zero, because reach-and-stop movements are usually accurate for healthy subjects. The mean error of this phase is typically defined as the *subject-dependent bias* of the task, and it is used to adjust the data collected in the other phases [85]. However, in this experiment the baseline phase is not long enough to ensure convergence of the error. For this reason, the subject-dependent bias was not used to correct the data of the other phases.

3. **Learning:** in this phase the visual rotation of the targets was applied and the subject had to adapt to this perturbation. With its 800 trials (400 outward and 400 inward), this was the longest phase of the experiment. For this reason, this phase was divided into ten blocks of 80 trials each to reduce fatigue. In this phase, the visual rotation was applied to all the subjects and the vibrotactile feedback was applied to the subjects in the vibration group. The data from these trials, called ***RV*** (Rotation Vibration) trials, gave us information about how quickly subjects improve their task performance. These trials alone were not enough to infer that the subject was learning an internal model that compensates the visual distortion. For these reason, two kinds of catch-trials were randomly but uniformly distributed across this phase of testing with a density of about one catch-trial every five trials. The first kind of catch-trials had the visual distortion but not the vibrotactile feedback (in the control group these catch-trials were exactly equivalent to normal trials) and they are called ***RnV*** (Rotation no Vibration) catch-trials. In the experiment there was a RnV trial every nine trials, and they were used to see if the information transmitted by vibration is an important cue for the subjects. In fact, if in the

vibration group there is no significant difference between the error in the RV trials and the error in the RnV trials, then the information given by the vibrotactile feedback is not really useful to the subject to compensate the visual distortion. The second kind of catch-trials had neither the vibrotactile feedback nor the visual distortion, and they are called ***nRnV*** (no Rotation no Vibration) catch-trials. In this experiment there is a nRnV catch-trial every twenty trials, and they were used to measure the formation of an internal model. In fact, learning an internal model that predictively compensate for the visual distortion will produce the same motor output on these appearance of these catch-trials because the catch-trials cannot be predicted. For this reason, the expected output of nRnV catch-trials is an error that gradually increases proportionally to the error decrease in RV trials.

4. **Generalization:** this phase was used to understand if the subject was able to generalize the internal model consolidated in the learning phase. In this phase each subject had to do 80 movements (40 inward and 40 outward) towards three outer targets whose positions were still on the circumference, but different from the positions used in the previous phases (Figure 21). These new targets give us the possibility to understand if a subject learned only a precise trajectory, or if he was able to learn the “structure” of the impairing visual deformation and if he was consequently able to compensate that deformation to reach any possible target.

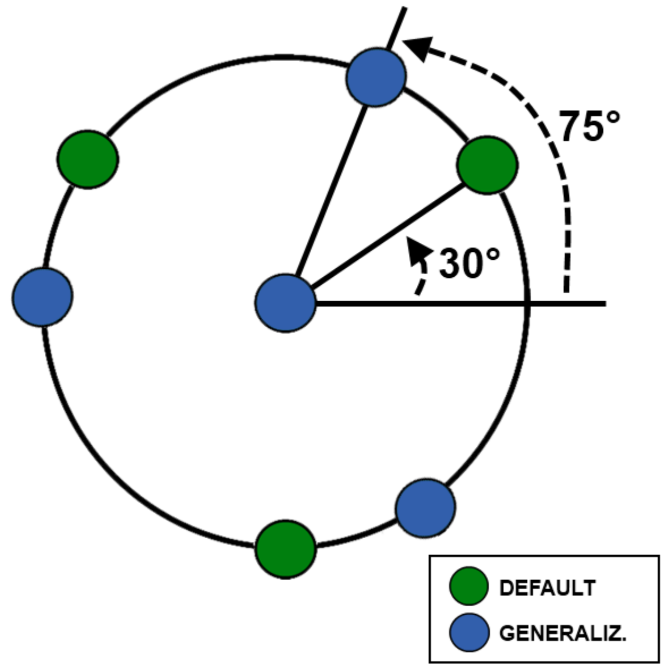

Figure 21: The targets of the generalization phase (blue) compared with the targets of the other phases (green). The targets of the generalization phase were equidistant and the angle of the first target was chosen equal to 75 degrees.

5. **Washout:** this is another phase that was used to understand if the subjects built an internal model to compensate the visual distortion. During the 160 movements of this phases (80 inward and 80 outward, divided into two blocks of 80 movements each) both the visual distortion and the vibrotactile feedback were removed. In this phase, if an internal model had been developed in the learning phase, it was possible to observe how the internal model was gradually readapted to the unperturbed reach-and-stop task. Ideally, the aim of this phase was to analyze how the effect of the nRnV catch-trials evolves when subjects were exposed for prolonged periods of time.

3.3 DATA ANALYSIS

In this section it is described how the data collected during the experiment was used to extract useful information. A huge amount of data was collected with a frequency of 100 Hz while each subject performed the experiment. A file of a typical experiment takes up about 30 Megabytes and it is in average 180,000 lines long. Each entry of these files contains the timestamp, the position of the subject's hand in the 3D workspace, the sensory feedback used and their intensities, and the error vector. In this section is described, at first, how this data are preprocessed to reject the outliers and some specific trials. Then, the features used to study the learning process are described. And finally the techniques used to perform the statistical analysis are described.

The data of the experiment was analyzed with MATLAB R2011a, R 2.14.1 and some custom applications written with Python 2.7.2.

3.3.1 Data preprocessing

The raw data collected during several sessions of the experiment contained information that needed to be rejected. Moreover, it was necessary to process this raw data to obtain more high level information, such as the movement velocity. In this section the criteria to clean the data and the methods to obtain more high level information are described.

3.3.1.1 2D Transformation

The coordinate system of the data collected during the experiment reflects the three-dimensional nature of the workspace. However, in Section 3.2 it is described that the subjects were performing a reach-and-stop task on a 2D plane, and the movements of the subjects were constrained to this plane by the robotic arm. For this reason, the component of the movement vector orthogonal to the plane can be ignored.

The unit of measurement of the original 3D coordinate system is in meters. Hence, if the distance between two points is equal to one, then in real world that distance is equal to one meter. This can be done because the VRROOM system was properly calibrated. It is suitable, during the transformation from the 2D system to the 3D system, to not modify this mapping between virtual world coordinates and real world coordinates. Instead, it is useful to change the origin of the coordinate system because in the 3D system it is far from the area where the targets are displayed.

Figure 22 describes the transformation from the 3D coordinate system (x, y, z) to the 2D coordinate system (u, v). The origin of the 2D system overlaps the center of the central target C (x_c, y_c, z_c) and does not have the component of the vector orthogonal to the plane.

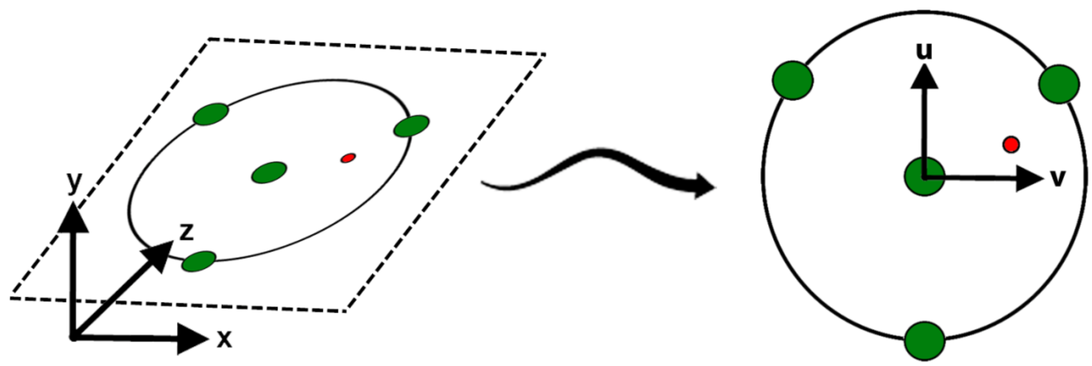

Figure 22: Transformation from the original 3D coordinate system $(\boldsymbol{x}, \boldsymbol{y}, \boldsymbol{z})$ to a 2D coordinate system $(\boldsymbol{u}, \boldsymbol{v})$. In the original 3D coordinate system the origin is far from the area where the targets are displayed, and the unit of measurement is in meters. This 3D system is transformed into a 2D system with the origin centered on the central target, and with the same unit of measurements of the 3D system. This transformation is obtained by eliminating the component orthogonal to the plane in the 3D system.

To perform the transformation from the 3D system to the 2D system, the following operations are performed:

1. The central target C is translated to the origin with the translation matrix T_{-C};
2. The axes of the 3D system are rotated to align with the 2D system using the rotation matrix R;
3. The component orthogonal to the plane is discarded.

With $T_{-C} = \begin{bmatrix} 1 & 0 & 0 & -x_c \\ 0 & 1 & 0 & -y_c \\ 0 & 0 & 1 & -z_c \\ 0 & 0 & 0 & 1 \end{bmatrix}$ and $R = \begin{bmatrix} u_x & u_y & u_z & 0 \\ v_x & v_y & v_z & 0 \\ n_x & n_y & n_z & 0 \\ 0 & 0 & 0 & 1 \end{bmatrix}$, where u and v are properly chosen orthogonal vectors from the center to the circumference and n is the normal of the plane.

Given a generic point $P\ (x_p, y_p, z_p)$ in the 3D space, the point $P'\ (u_p, v_p)$ in the 2D space is calculated as follows:

$$P'\left(u_p, v_p, n_p\right) = R \cdot T_{-C} \cdot\ P\ (x_p, y_p, z_p)$$

And the component n_p is discarded.

3.3.1.2 Resampling

The VRROOM workstation collected data with a sampling frequency of 100 Hz. However, an analysis of the raw data showed that the sampling time is not constant (Figure 23).

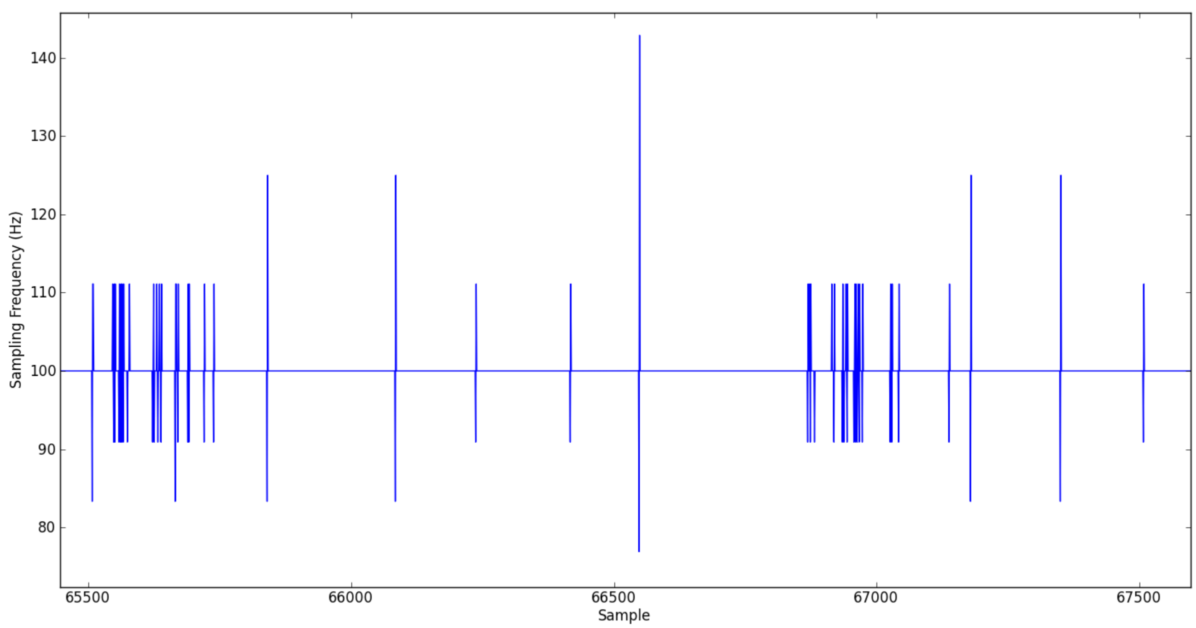

Figure 23: The VRROOM workstation is supposed to collect data with a constant sampling frequency of 100 Hz. However, the analysis of the raw data shows that the sampling frequency is not constant. This image shows how the frequency changes during the sampling of about 2,000 samples.

For this reason, it was necessary to resample the raw data at the average frequency of 100 Hz. This process was done with the method of *linear interpolation*.

3.3.1.3 Velocity

After the coordinate system transformation and the resampling, it is possible to use the data to calculate the velocity of the hand. This velocity is used to understand which parts of a movement should be used to extract features.

The velocity is calculated as the difference between consecutive positions of the hand divided by the time elapsed between these two positions. Figure 24 shows that the velocity calculated with this technique is quite noisy, with huge spikes that increase the variance of the data. To reduce the sampling noise a Gaussian Mobile Filter is applied.

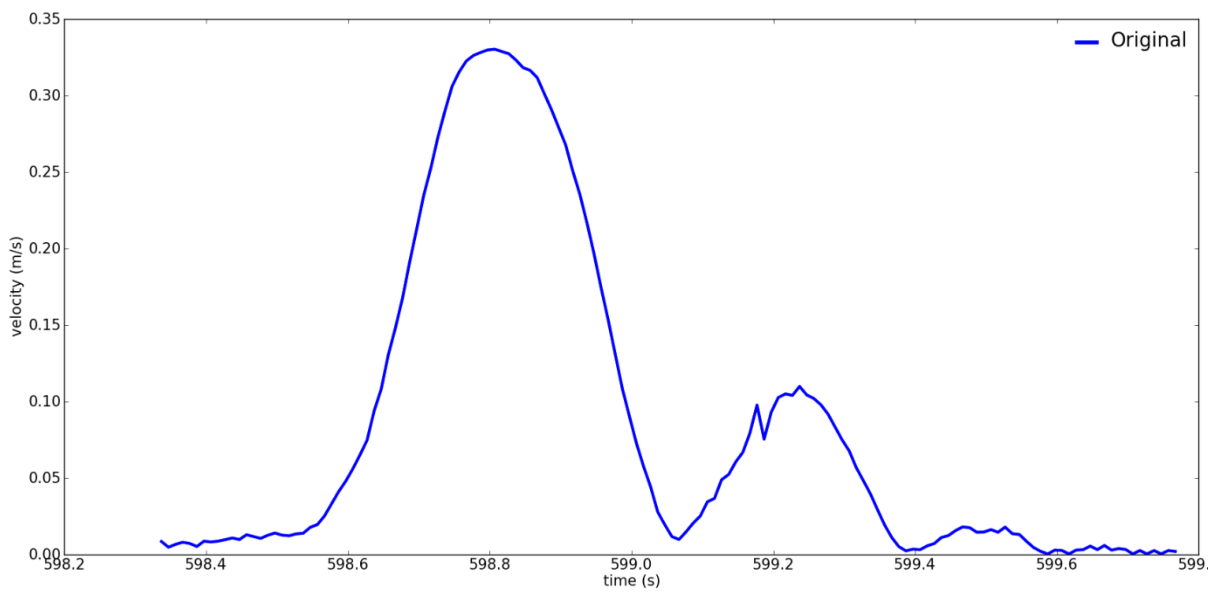

Figure 24: Movement velocity calculated from the data without the use of any technique to reduce the noise.

It is possible to obtain better results if a low-pass filter is applied. In fact, it is commonly accepted that the human component in the hand velocity occupy frequencies not higher than 7 Hz. For this reason, it is possible to clean the velocity data without the risk of removing useful information with a Gaussian Mobile Filter whose cut-off frequency is 21 Hz. A Gaussian Mobile Filter substitutes the value of each point with a weighted sum of the values of all its neighbors inside a given window. The weights are given by a Gaussian distribution centered on the point whose value is going to be substituted. Figure 25 shows the result obtained by applying the Gaussian Mobile Filter on sample data.

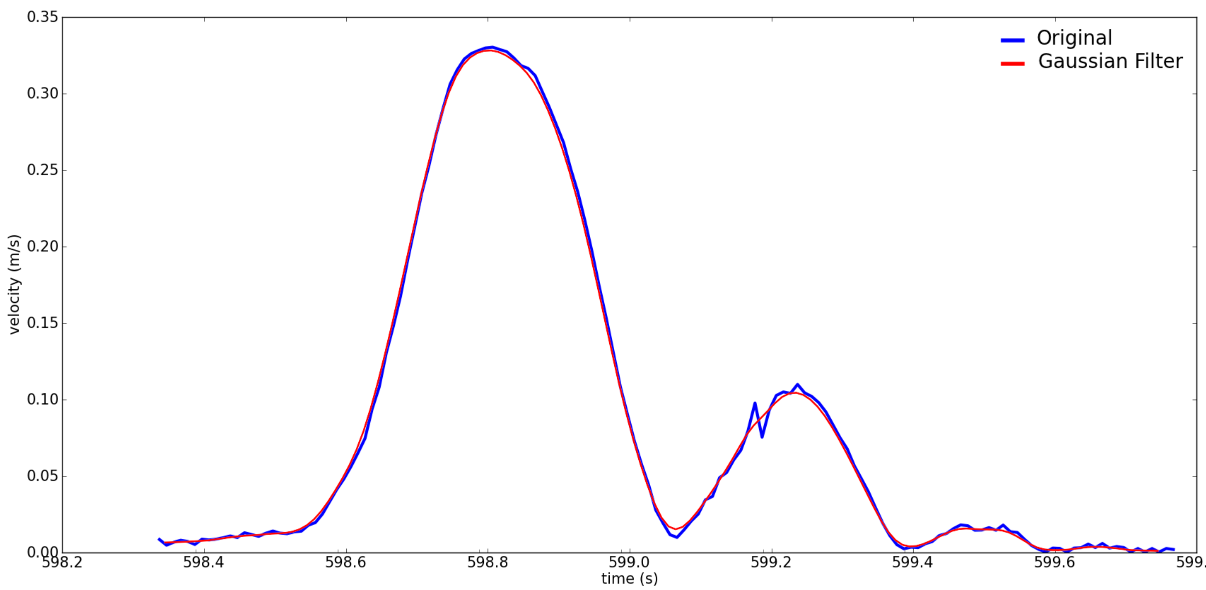

Figure 25: The velocity data cleaned with a Gaussian Mobile Filter whose cut-off frequency is 21 Hz. The cut-off frequency was chosen to be three times 7 Hz, because all the human components in the hand movements are below this threshold.

3.3.1.4 Data rejection

The criteria to reject data collected during an experiment session can be divided into two level of granularity: criteria to reject all the data of an entire movement and criteria to reject part of a valid movement's data. In the former case, a whole movement was removed because it was not useful to extract data or it could introduce relevant noise into the results. In the latter case, some parts of a movement did not contain useful information, and for this reason they were removed.

If we consider the data at the granularity of whole movements, then a movement was rejected if:

1. **The movement is an *inward movement***: all the movements from the external targets to the central one are not used. The inward movements are easier that the outward one, and for this reason the performance for these two kinds of movements cannot be evaluated together;

2. **The movement is after a catch-trials or a rest**: movements after catch-trials and rest are significantly different from other movements [86]. For this reason, six movements (three outward and three inward) after each catch-trial and four (two outward and two inward) after each rest are rejected.

3. **The subject started moving in the direction of a wrong target:** the targets were displayed in random order to the subjects to avoid predicting the location of subsequent targets. However, the subjects still tried to predict target locations, and this lead to "false starts" in the direction of the target that the subject believed to be the next. These movements were discarded because the subjects, when they realize that their movement

is towards a nonexistent target, introduce a huge error in their attempt to correct the trajectory (Figure 26).

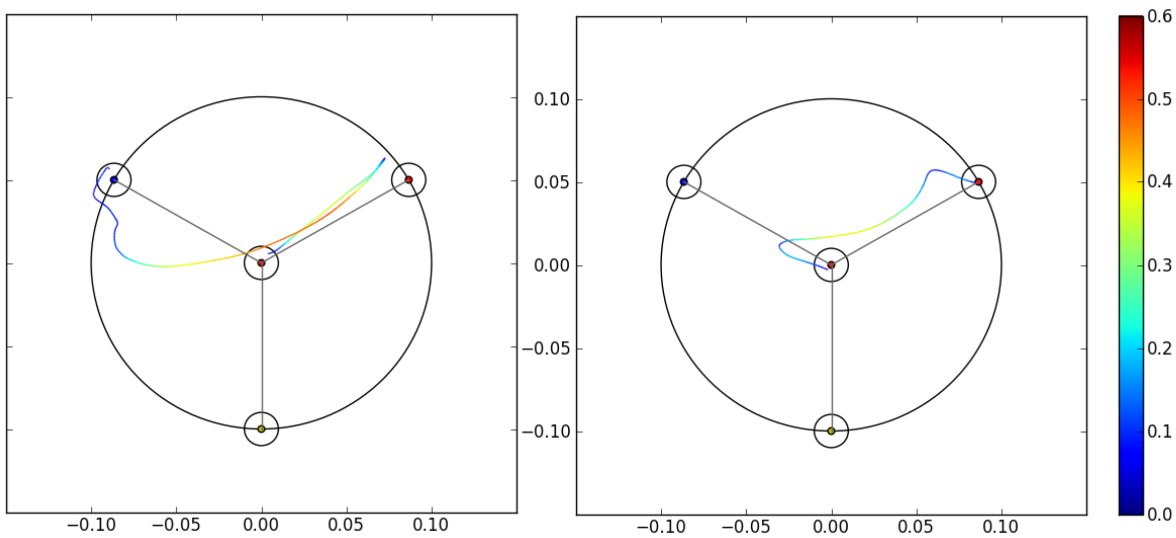

Figure 26: Examples of trajectories where the subject started moving towards the wrong target. These trajectories were rejected because the error done by the subject is higher of the error that normally is done. The color of the trajectory indicates the velocity of the hand and goes from dark blue (0.0 m/s) to dark red (0.6 m/s).

4. **The movement is extremely slow:** a movement was rejected if the velocity was below 0.1 m/s for the whole movement. This threshold defined a slow movement, and it is possible to assume if this velocity was never exceeded that the movement was almost entirely dominated by the feedback component. Hence, the error in this movement is lower than the average.

After the rejection of invalid trajectories, it was necessary to extract from the valid ones the movement part that was significant. Fast reach-and-stop movements, like the ones done in this experiment, are ballistic movements. A ballistic movement is defined as muscle contractions that exhibit high velocities over a short period of time. A velocity vs. time graph, such as Figure 27, shows these movements as having a bell-shaped form.

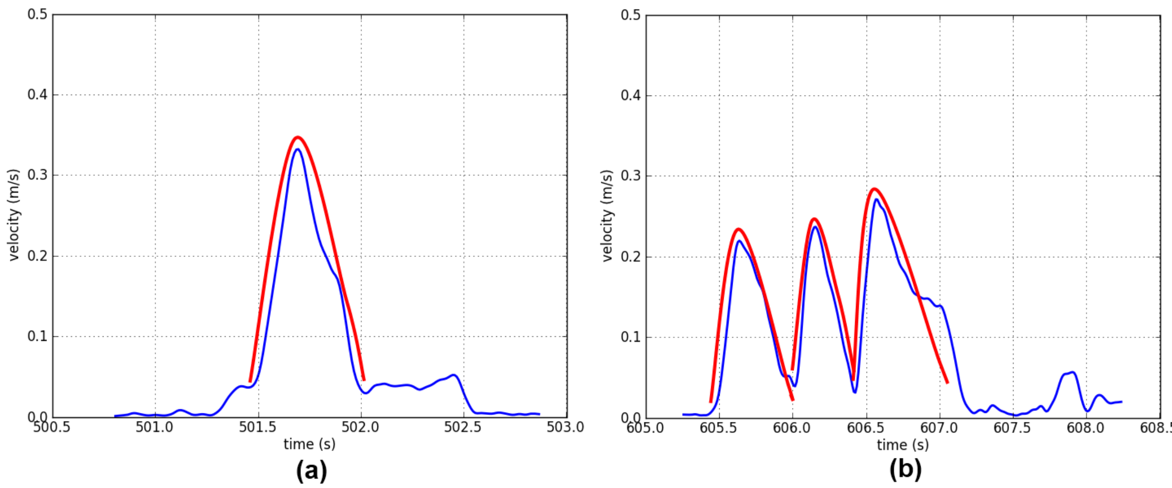

Figure 27: Decomposition of two reaching movements (blue) into ballistic movements (red). Trajectory (a) is formed by only one ballistic movement, while trajectory (b) is formed by the overlapping of three ballistic movements. Multiple ballistic movements in a single trajectory imply that in between the subject's CNS is correcting the movement, and it is not possible to exclude that it is using a feedback control system.

A typical reach-and-stop movement of a healthy subject is made up of a single ballistic movement. In fact, this is a simple task and the central nervous system (CNS) is able to calculate the muscle activation pattern needed to reach the target without the need of on-line corrections. Instead, the CNS requires some corrections of the trajectory when the subject must deal with a perturbation that cannot be predicted well. In this case, the CNS uses the activation pattern that is believed to be optimal; subsequently, when the first sensory stimuli arrive in the CNS, it will evaluate the performance and transmit a new and activation pattern. For this experiment, it is more interesting to analyze the data of the first activation pattern or initial ballistic movement, because it is likely determined only by the internal model and not by on-line corrections.

The algorithm used to robustly extract the first ballistic movement is described as follows:

1. Set a static threshold Th_{static} which indicates a low level of velocity that is above the initial high frequency noise. The threshold Th_{static} was chosen equal to 0.1 m/s.

2. Find the first local maximum V_{max} above Th_{static} and the first local minimum V_{min} below Th_{static}. A local maximum is preferred to a global maximum because one of the follow-up ballistic movements could have a peak velocity higher than the one of the first ballistic movement.

3. Calculate the dynamic threshold $Th_{dynamic} = 0.20 * (V_{max} - V_{min}) + V_{min}$. This threshold is equal to the 20% of the distance between V_{min} and V_{max}.

4. The first ballistic movement is made up of all the samples from V_{max} going backwards until the first sample below $Th_{dynamic}$ and from V_{max} going forward until the first sample below $Th_{dynamic}$ is reached.

Figure 28 shows the output of the algorithm applied to two trials of the dataset.

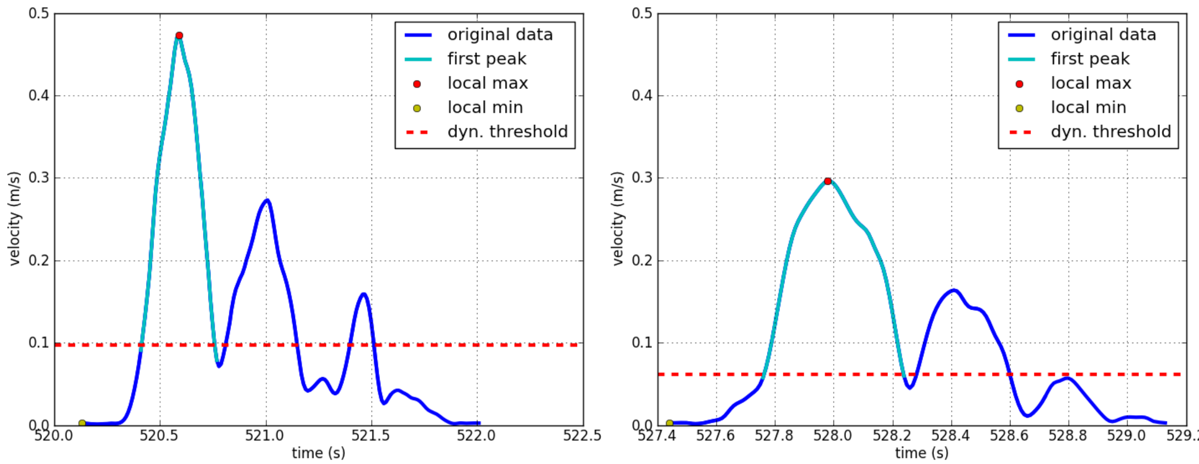

Figure 28: Algorithm to extract the first ballistic movement (cyan) from an entire trajectory (blue). The red dot is the local maximum above the static threshold, the yellow dot is the local minimum below the threshold and the red dotted line is the dynamic threshold.

3.3.2 Features

Once the trajectory had been successfully cleaned, the next step was to extract some relevant features which allowed us to compare the learning process between different subjects. The features used were four and are described in the following sections: maximum perpendicular distance, error in the initial direction of movement, learning index and execution time. Among these four features, the most interesting one is the *maximum perpendicular distance*, because it indicates how far the movement is from the ideal. The *initial direction of movement* was extremely useful to identify trajectories that should have been rejected. The *learning index* is a useful indicator that returns a normalized value which is independent from perturbation intensity and subject. Lastly, the execution time gives information about the time required to perform a reaching movement.

3.3.2.1 Maximum perpendicular distance

Given a trajectory AB that travels from point A to point B and a position H along the trajectory, then the error vector ē, which connects point P to point H, is called ***perpendicular distance***; where P is the orthogonal projection of H on the straight line that connects A with B (Figure 29).

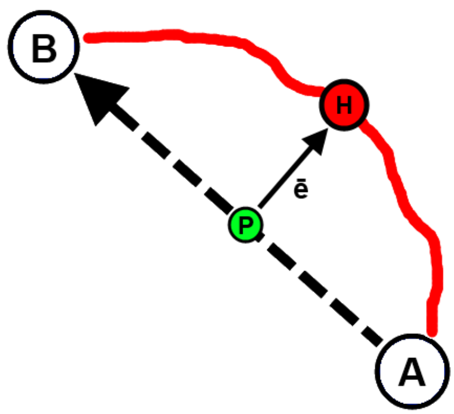

Figure 29: Perpendicular distance of a point H along a trajectory from the point A to the point B. The perpendicular distance of the point H (vector ē) is the vector between H and its orthogonal projection P on the straight line that connects A with B. The maximum perpendicular distance of a trajectory is the maximum perpendicular distance along that trajectory.

Given the unit vector $\widehat{\boldsymbol{M}} = \frac{B-A}{|B-A|}$ and the vector $\boldsymbol{T} = B - H$, the projection of $\boldsymbol{T}$ onto the unit vector $\widehat{\boldsymbol{M}}$ is equal to $\widehat{\boldsymbol{M}}(\boldsymbol{T} \cdot \widehat{\boldsymbol{M}})$. Hence, the orthogonal projection of point P onto AB is $P = B - \widehat{\boldsymbol{M}}(\boldsymbol{T} \cdot \widehat{\boldsymbol{M}})$, and the perpendicular distance is the magnitude of the vector $\boldsymbol{E} = H - P$.

The ***maximum perpendicular distance*** (known also as uniform norm or Chebychev norm) along a given trajectory is the maximum value of perpendicular distance along that trajectory.

It is important to point out that the magnitude of the perpendicular distance is the value used to modulate the vibration amplitude during the learning phase of the experiment.

3.3.2.2 Initial direction error

It is particularly interesting for the aim of this experiment to analyze the first phase of the movement, because it best reflects the operation of a feedforward controller based on an internal model of the environment dynamics. The initial path of movement reflects this early movement phase by forming a vector from the start point to the position of the hand after 100 milliseconds (Figure 30a).

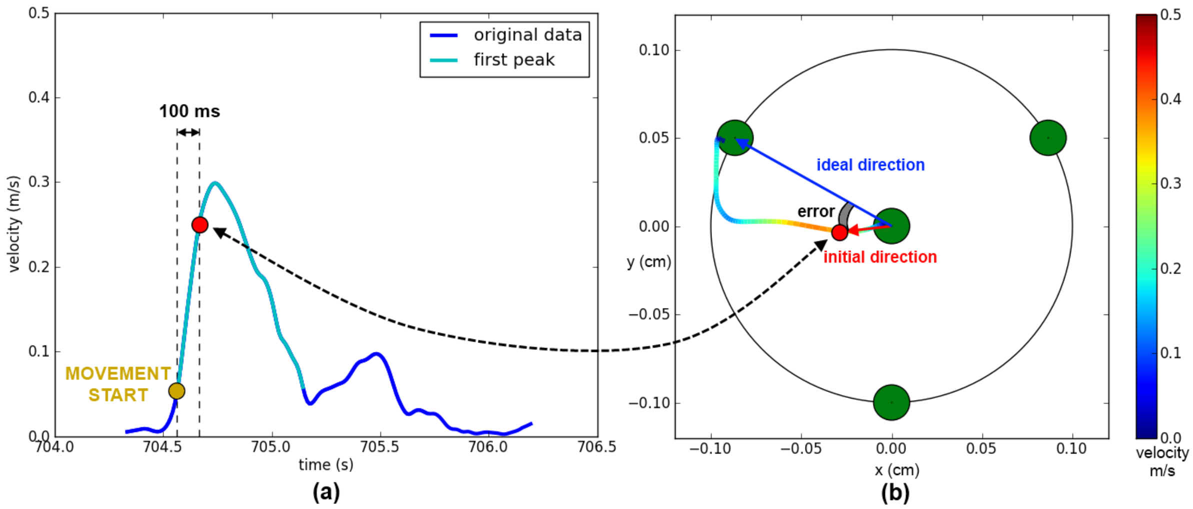

Figure 30: The initial direction error between the initial direction of movement and the ideal one. Figure (a) shows that the point P selected to calculate the initial direction is 100 milliseconds after the movement's starting point S. S is the beginning of the first ballistic movement. (b) shows that the initial direction error is the angle between the initial direction vector P-V and the vector that connects the end target and the start target.

The initial direction error is the angle between the initial direction vector and the vector that connects the end target with the start target (Figure 30b). The convention chosen for this feature assigns a positive value for counterclockwise errors, for this reason the range values for these errors is ±180°.

3.3.2.3 Execution Time

The Execution Time (ET) is calculated as the time required to execute the first ballistic movement. In this way, it is not taken in consideration an eventual delay at the beginning of the movements.

3.3.2.4 Learning index

As previously discussed, the CNS can reduce the error caused by the perturbation at least in two different ways. The first method is a feedback control which uses the sensorial inputs. Ideally, this stabile feedback system will reduce the errors in the RV trials. However, in such a system errors will not be present when the disturbance is removed during the nRnV catch-trials. Alternately, learning an internal model of the perturbation will also result in a reduction in errors during the RN trials. However, this strategy will produce large errors in the nRnV catch-trials, and these errors should be proportional to the amount of time spent to update the internal model [85,87].

The distance between the nRnV error curve and the RV error curved correspond to the effect size of perturbation on the error (Figure 31). This effect size depends on the magnitude of the perturbation and on subject-specific characteristics, such as the length of the arm. In the experiment described in this document, the magnitude of the perturbation (the angle of rotation) is held constant across subjects. However, the subject-dependent characteristics are, by definition, different from subject to subject. Hence, it is interesting to use the effect size as normalization value to obtain a measure of learning independent from the effect size. This normalized value is called learning index [85,87].

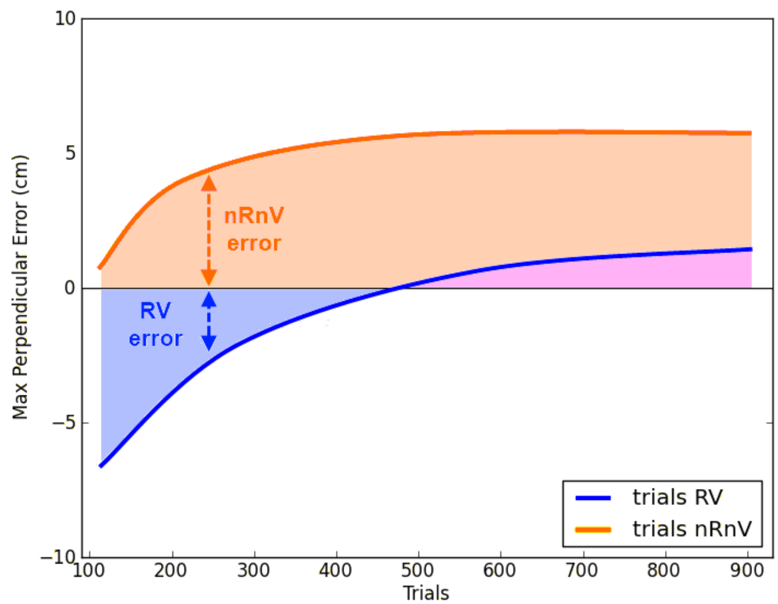

Figure 31: The learning index is used to calculate a feature that is invariant to the effect size. This size depends on the perturbation's magnitude and on the subject dependent variables. The effect size is equivalent to the distance between the nRnV and the RV error curves; in this case, the error used is the maximum perpendicular error. The learning index is defined as the normalization of the error with the effect size.

For example, in Figure 31 it is shown a plausible drawing of the RV and nRnV error curves with the error calculated as maximum perpendicular error. Because the nRnV curve is always above the other one, the effect size can be calculated for each trial T with the following formula:

$$effect\ size_T = \left|error_{T,\ nRnV} - error_{T,\ RV}\right|$$

Now, it is possible to calculate the learning index of the error. For example:

$$learning\ index_{T,\ nRnV} = \frac{error_{T,\ nRnV}}{effect\ size_T} = \frac{error_{T,\ nRnV}}{\left|error_{T,\ nRnV} - error_{T,\ RV}\right|}$$

It is important to point out that in the experiment described in this document, the learning index should not be considered as the main measure of learning due to the small number of nRnV catch-trials. This limited number of trials entails a too high granularity in the nRnV curve, which leads to an higher sensibility to noise especially at the beginning of the curve. It was not possible to increment the number of nRnV catch-trials because a second set of catch-trials (RnV trials) is present in the learning phase, and a higher number of catch-trials hampers the normal trials.

3.3.3 Learning model

The features of each subject's learning phase were fitted to an exponential model, to study how the subjects of the vibration group are affected by the vibrotactile stimulation. The exponential curved used is

$$A + Be^{-\frac{t}{C}}$$

where A is a plateau reached during the learning phase, B is how much the error changed from the beginning of the learning phase to the end and C is the dominant time constant for the error to decrease. This model has been used multiple times in the literature [5,7,8,9,10,20,69,85], and typically A is called *learning offset*, B is called *amount of learning* and C is called *learning rate*.

The learning rates and the learning amounts for the vibration treatment group will be compared to the control group to test the hypotheses that vibration speeds up and enlarges the amount of learning over controls. Moreover, it is possible to use this exponential model to verify some secondary hypothesis, such as that vibration became an important cue for the control group.

3.3.4 Statistical analysis

To compare the effects of vibration, two general methods were used. The first approach is to calculate the average of a subject's performance feature (e.g. Maximum Perpendicular Error) over some consecutive trials. This approach was typically used to estimate the difference between two distinct points onto the learning curve; for example the difference between the Maximum Perpendicular Error (MPE) that a subject's trajectory produced at the beginning and end of the learning phase. The second method was used to compare entire learning curves. The trial-by-trial data along each curve was regressed into an exponential function $A + Be^{-\frac{t}{C}}$, where A is the plateau, B is the amount of change and C is the dominant time constant. The advantage of this approach is that it summarizes the properties of a learning curve in only three parameters, but the drawback is the intrinsic error of the regression. This fitting imprecision is particularly evident if there is a high variance in the dataset.

T-tests were performed to calculate the significance of an effect. These tests were run assuming an unknown distribution's mean and variance. If the tests were run between two different independent distributions, then the variances of these distributions were assumed distinct from each other and unknown. Accordingly with the kind of effect, either a two tailed or a one tailed t-test was run. It was not necessary to run ANOVA tests because it had never been necessary to compare more than two independent populations. The significance for all statistics is $\alpha = 0.05$.

Lilliefors tests were run when it was necessary to check if a set of data was significantly different from an unknown Gaussian distribution.

The effect size between two populations was estimated with the Cohen's effect size d, which is defined as the difference between the means of the two populations divided by the standard deviation of the data:

$$d = \frac{\bar{x}_1 - \bar{x}_2}{s}$$

CHAPTER 4:

RESULTS

In this Chapter are described the results of the data analysis. First, a general description of the trajectories and of the learning curves during the different phases of the experiment is discussed. This general description is used to give a high level overview to the reader. Then, the data of each phase is analyzed to extract relevant information. This information is used in Chapter 5 to discuss the results.

4.1 TRAJECTORIES AND LEARNING CURVES

In this section a description is given of the learning curves and of the trajectories of typical subjects. This section is used to give an overview of their general structure. A more detailed and technical description is provided in the following sections.

To provide a general view of the trajectories that were usually found in each of the experiments the reader is directed to Figure 32 which shows the trajectories of two typical subjects (one subject of the vibration group and one subject of the control group) in the six distinct experimental conditions. ***Baseline*** shows the first ten outward movements performed during the baseline phase, where subjects had to reach the targets without the vibrotactile feedback and the rotation of the visual field: the trajectories are straight and the perpendicular error is minimal. ***Early Learning*** and ***Late Learning*** shows, respectively, the first ten movements and the last ten movements of the learning phase, where the visual distortion is applied and the vibration group receives the vibrotactile feedback. At the beginning of this phase the trajectories are extremely biased by the visual rotation, but gradually the subjects corrects the movements until reaching a nearly straight movement. ***Generalization*** shows the first ten movements of the generalization phase, where the vibration group did not have any more the vibrotactile feedback, the visual distortion is still present but the targets are in naïve locations. Finally, ***Early*** and ***Late Washout*** shows, respectively, the first ten and the last ten movements of the washout phase, where neither the vibration nor the visual distortion are present. The subjects show a high error at the beginning of this phase that is gradually reduced.

The perpendicular error of the trajectories plotted in Figure 32 is high at the beginning of the learning phase, but it decrease as the number of trials increase. During the generalization phase the error remains relatively small. The error increases when, in the washout phase, the perturbation is removed; notice that the error in the Early Washout is in the opposite direction of the error in the Early Learning phase.

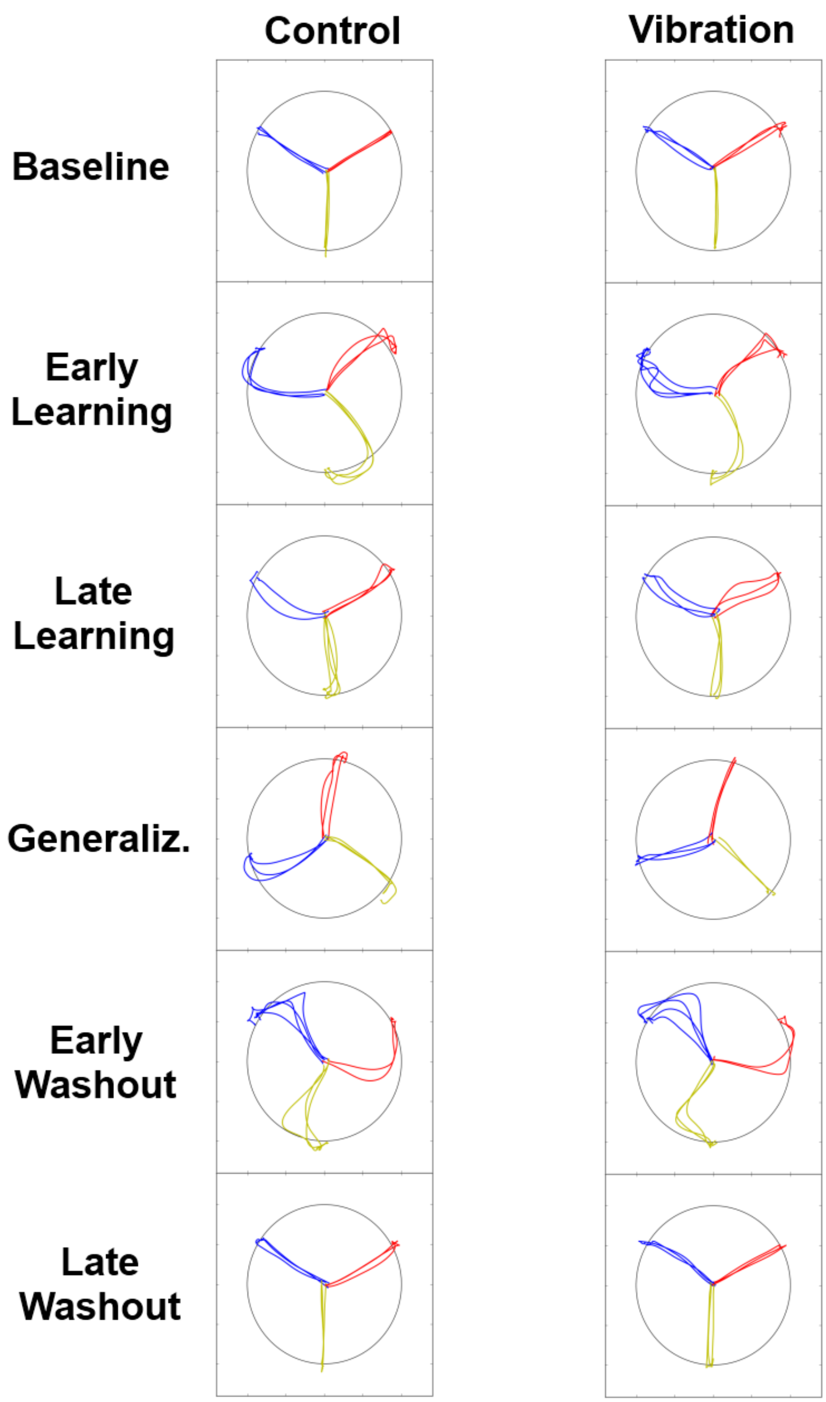

Figure 32: Cursor's trajectories of different phases for two typical subjects. With "early" is intended the first ten trajectories of a phase, and with "late" is intended the last ten trajectories of a phase.

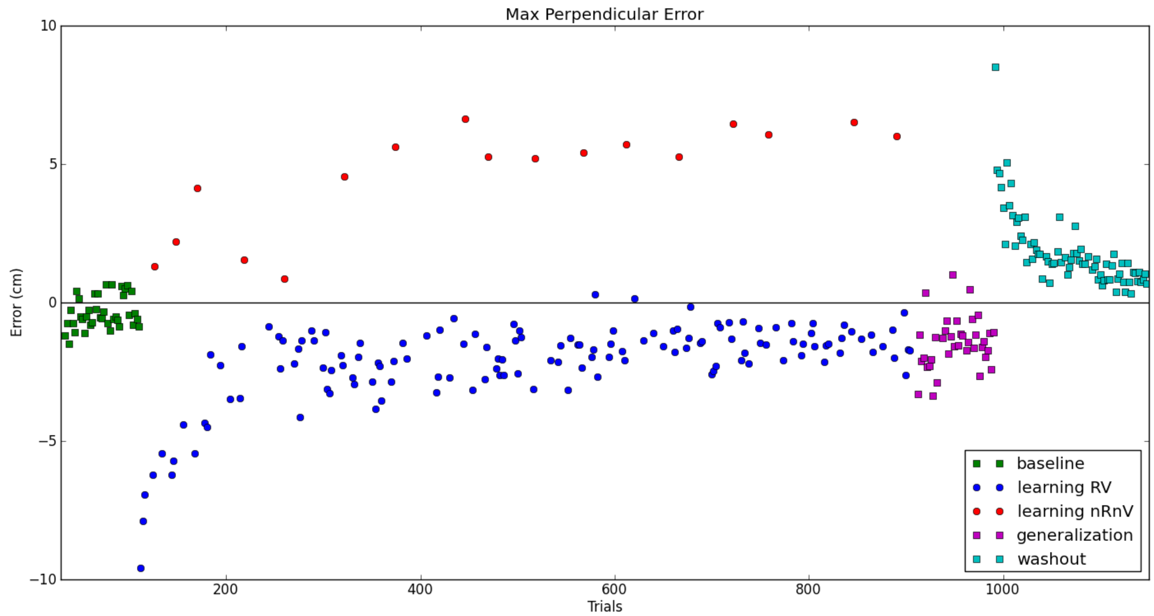

Figure 33: Plot of the Maximum Perpendicular Error of a typical subject. Each subject had a plot which resembles this one. In the learning phase are plotted the MPE of both RV trials and nRnV catch-trials.

A similar trend in the perpendicular error is observed in all the subjects, and it is better depicted in Figure 33. This plot shows the time course of these error changes. The error decrease during the learning phase follows a rising exponential curve which reaches its asymptote at the end of this phase. While the error of the RV trials decreases, the error of the nRnV *catch-trials* increase. Finally, in this Figure the error of the washout phase is opposite to the error found in the learning phase and is almost the same initial magnitude, but in the opposite direction, as found in the beginning of the learning phase.

In the following sections, each phase is analyzed to show the statistical results of this experiment.

4.2 BASELINE

During the baseline phase the subjects of both groups were exposed to the same conditions: no distortion and no vibrotactile feedback. Moreover, healthy subjects are supposed to easily perform the task of this phase. For these two reasons, it was expected to have in both groups a constant performance along the entire phase and no difference between the performance of the two groups.

4.2.1 Maximum Perpendicular Error

Figure 34 shows the Maximum Perpendicular Error (MPE) in the baseline phase of both the vibration group and the control group. The dark green line represents the trial-by-trial mean of each group and the light green area represents the standard deviation of this mean. The red dotted line represents the mean of all the trials' MPE of each group.

For each subject, the difference between MPE of the first ten trials and of the last ten showed no significant difference from 0. Hence, in both groups the MPE is stationary during the entire baseline phase. Because the MPE is stationary, the overall MPE during the baseline phase of each subject was calculated; no significant difference between the means of the two groups was found.

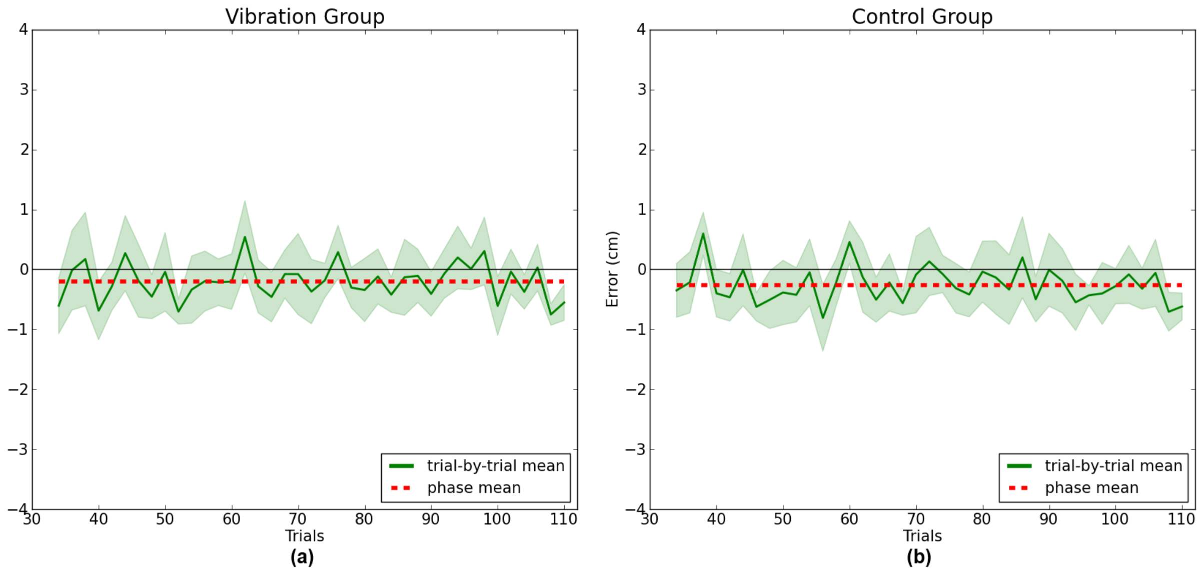

Figure 34: Maximum Perpendicular Error (MPE) in the baseline phase of each group. The light green area is the standard deviation, and the red dotted line is the average of the group

However, the overall means of each group were both significantly different from 0 ($p<0.05$). The mean of the vibration group is -0.2323 cm and the mean of the control group is -0.2776.

4.2.2 Execution Time

Figure 35 shows the Execution Time (ET) in the baseline phase for each group. The green line represents the trial-by-trial mean of each group and the light green area represents the standard deviation of this mean. The red dotted line represents the means of all the trials' ET for the two groups, with the mean of the vibration group equal to 0.3629 seconds and the mean of the control group equals to 0.3717 seconds.

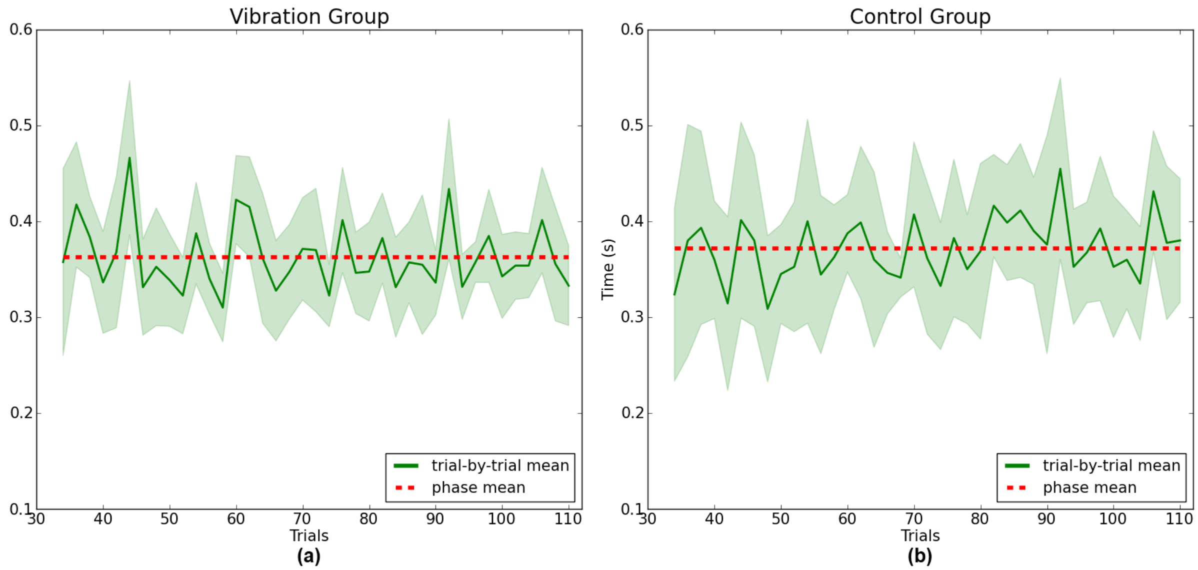

Figure 35: Execution Time (ET) in the baseline phase of each group.

For each subject, the difference between the first ten trials and the last ten trials of the baseline is not significantly different from 0. Hence, in both groups the ET is stationary along the whole phase but there is no significant difference between these means.

4.2.3 Initial Direction of Movement

Figure 36 shows the Initial Direction of Movement (IDM) in the baseline phase of each group. The green line represents the trial-by-trial mean of each group and the light green area represents the standard deviation of this mean. . The red dotted line represents the means of all the trials' IDM for the two groups, with the mean of the vibration group equal to 1.025 degrees and the mean of the control group equals to 1.207 degrees.

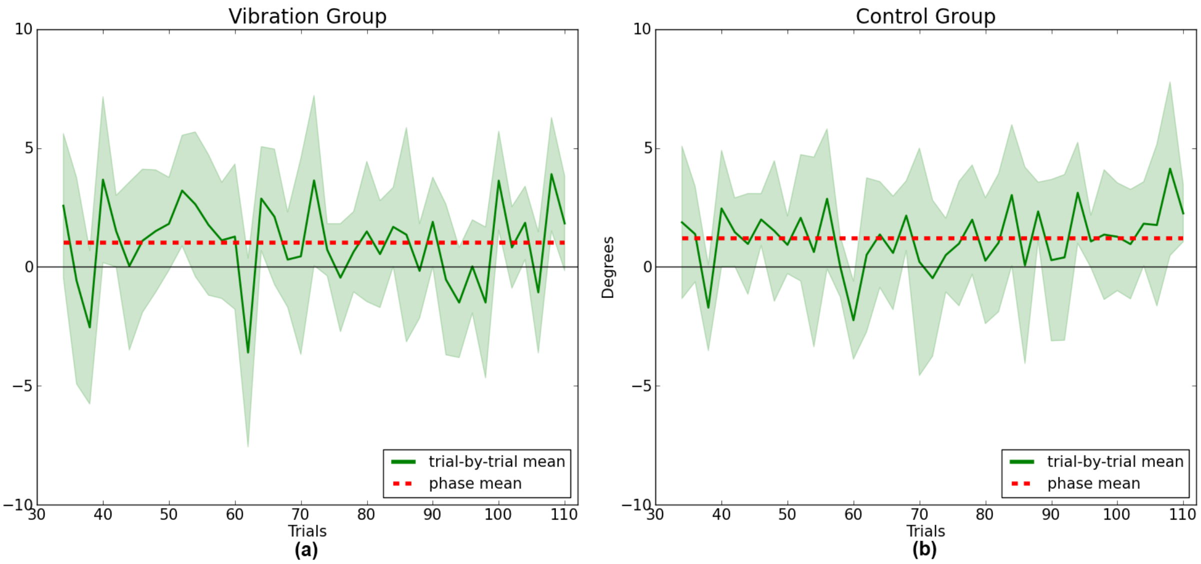

Figure 36: Initial Direction of Movement (IDM) in the baseline phase of each group.

For each subject, the difference between the first ten trials and the last ten trials of the baseline showed no significant difference from 0. Hence, in both groups the IDM is stationary along the whole phase but there is no significant difference between the these means.

4.3 LEARNING PHASE

As previously mentioned in Chapter 3, in this phase there were three kinds of trials. Figure 37 depicts the Maximum Perpendicular Error of each of these trials. The RV trials are the main trials of this phase: the vibration group has the visual distortion and the vibrotactile feedback, while the control group has only the visual distortion. The nRnV catch-trials are used to evaluate the amount of learning: in these trials there is neither vibration feedback nor visual distortion. Finally, in the RnV catch-trials there is the visual distortion but not the vibrotactile feedback. Obviously the RnV catch-trials are equivalent to the RV trials for the control group. This figure is useful to show the trend found in each kind of trial. In the following sections each kind of trial is analyzed.

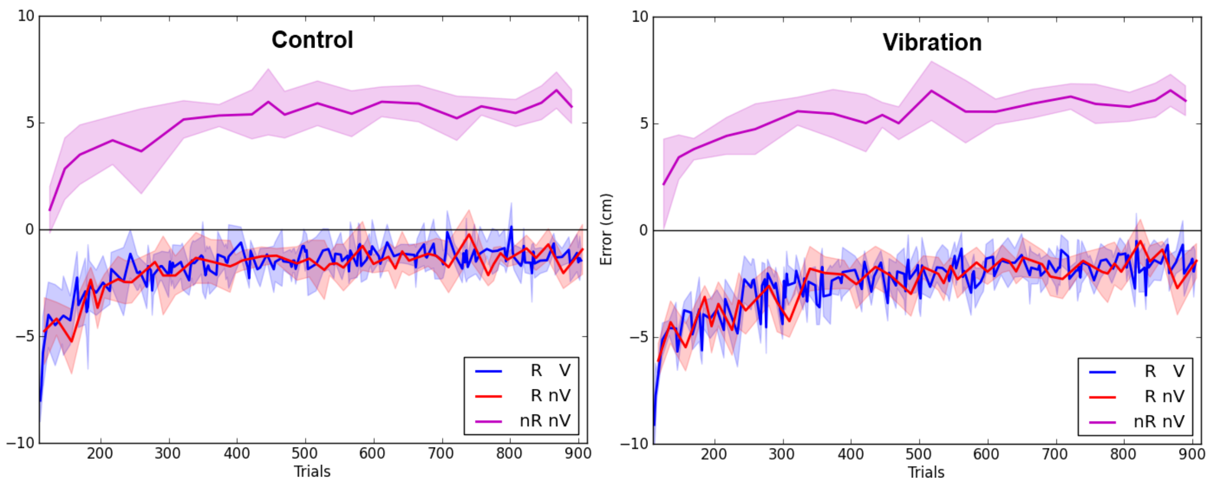

Figure 37: Maximum Perpendicular Error of the learning phase subdivided into the three distinct kinds of trials. The light colored areas are the standard deviation.

Due to the high number of observations that can be done on the learning phase's data, this section is divided into two main sub-sections. First, it is analyzed the performance within group, and after is analyzed the performance between groups.

4.3.1 Performance within groups

4.3.1.1 RV trials

Figure 38 depicts how the RV trials' MPE changes during the learning phase. In this figure, the blue line represents the variation in mean performance for subjects of the same group on a trial-by-trial basis, while the light blue area represents the standard deviation of this mean. For both groups, the difference between the average of the last ten RV trials and the average of the first ten RV trials of this phase is significantly greater than 0 ($p < 0.001$). Hence, the RV trials' performance significantly ***improved*** during this phase in both groups.

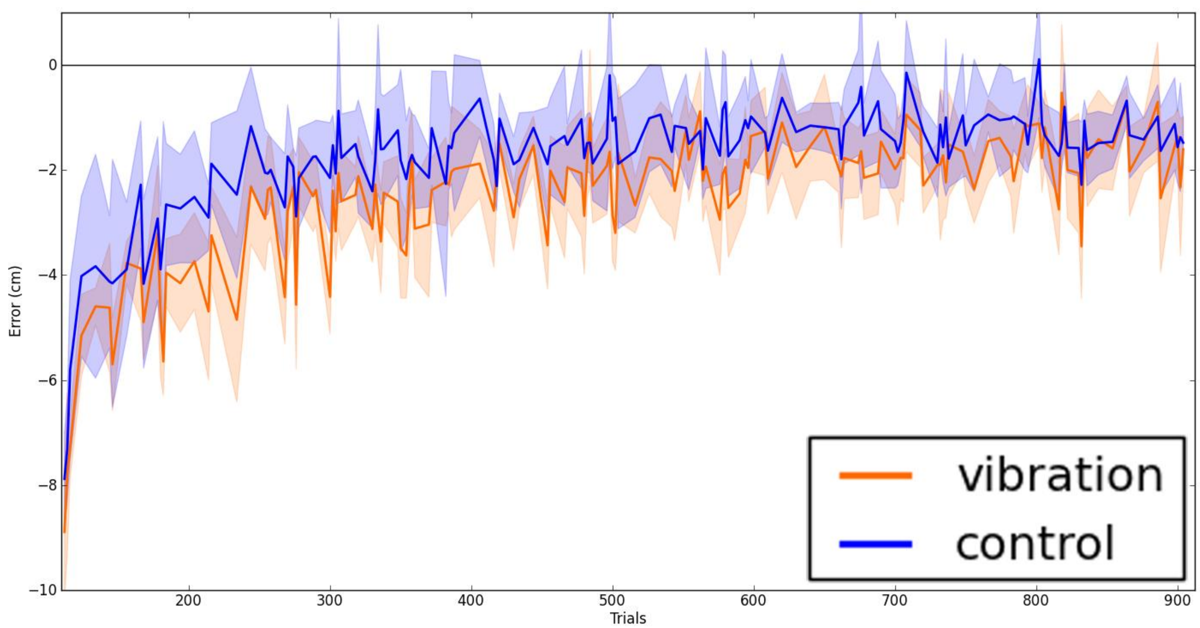

Figure 38: RV trials' Maximum Perpendicular Error (MPE) of each group in the learning phase. The light colored areas are the standard deviations.

Similarly to the previous figure, Figure 39 illustrates how the RV trials' ET changes during the learning phase. For both groups, the difference between the average of the last five RV trials and the average of the first five RV trials of this phase is significantly greater than 0 ($p < 0.05$). Hence, the RV trials' execution time significantly ***decreased*** in both groups during this phase.

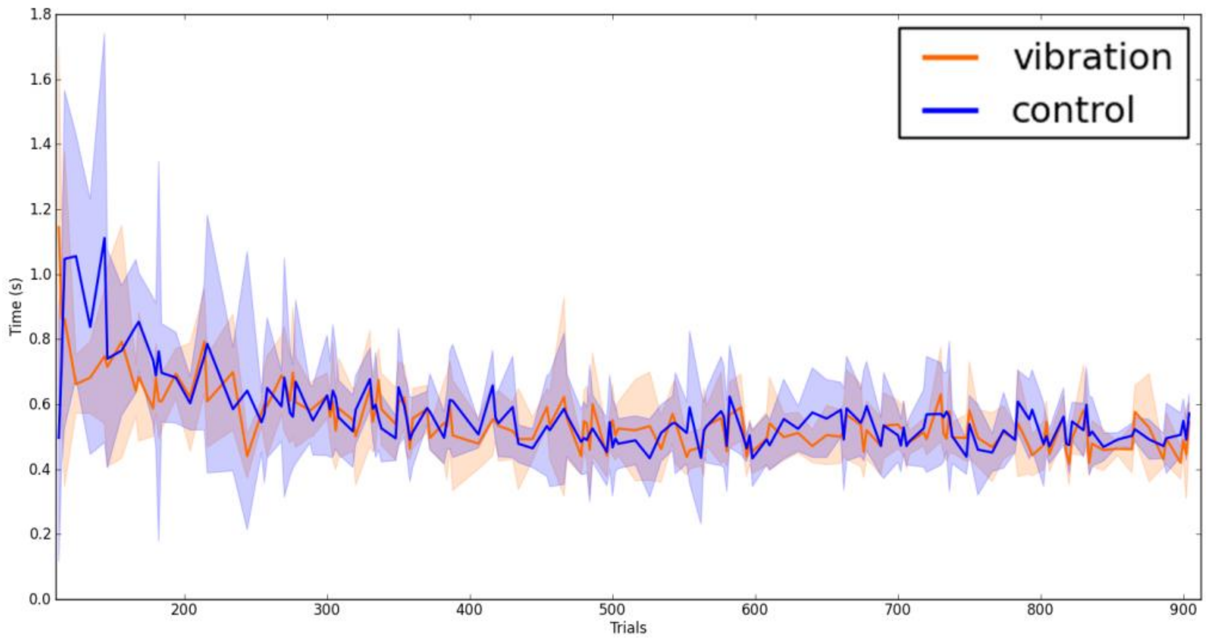

Figure 39: RV trials' Execution Time (ET) of each group in the learning phase. The light colored areas are the standard deviations.

4.3.1.2 RnV trials

Figure 40 shows the RnV catch-trials' MPE. Similarly to the previous test, an analysis was done on the difference between the first five trials and the last five trials. This difference was significantly greater than 0 ($p < 0.001$). Hence, also the RnV catch-trials' performance significantly ***improved*** during the learning phase.

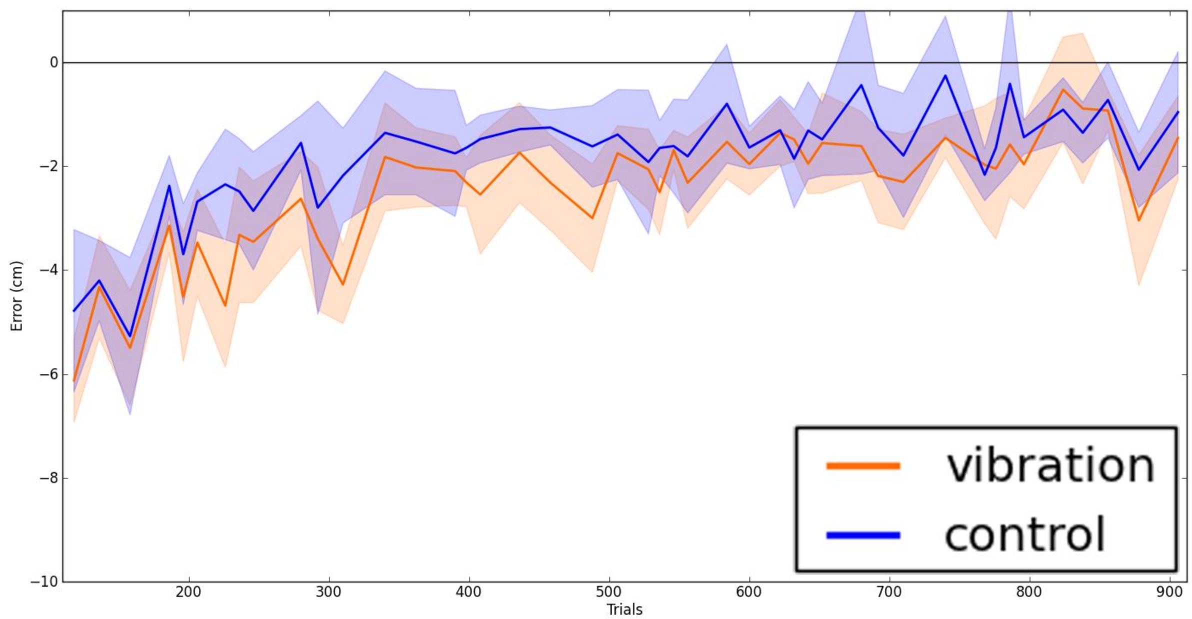

Figure 40: RnV catch-trials' Maximum Perpendicular Error (MPE) of each group in the learning phase. The light colored areas are the standard deviations.

Similarly to the previous image, Figure 41 illustrates how the RnV catch-trials' ET changes along the learning phase. For both groups, the difference between the average of the last five RnV trials and the average of the first five RnV trials of this phase is significantly greater than 0 ($p < 0.05$). Hence, the RnV catch-trials' Execution Time significantly ***decreased*** in both groups along this phase.

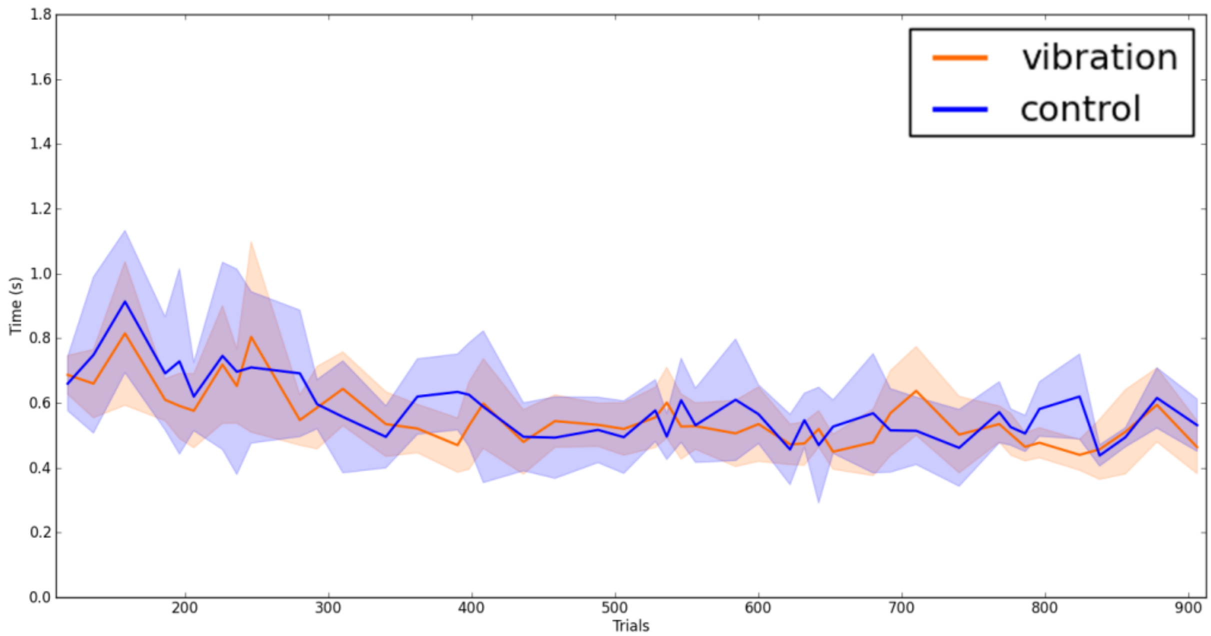

Figure 41: RnV catch-trials' Execution Time (ET) of each group in the learning phase. The light colored areas are the standard deviations.

An analysis was performed to examine if there is a significant difference between the RV trials and the RnV catch-trials. To perform this analysis, the exponential regression of each subject is calculated, and the RV parameters are compared with the RnV parameters (Figure 42).

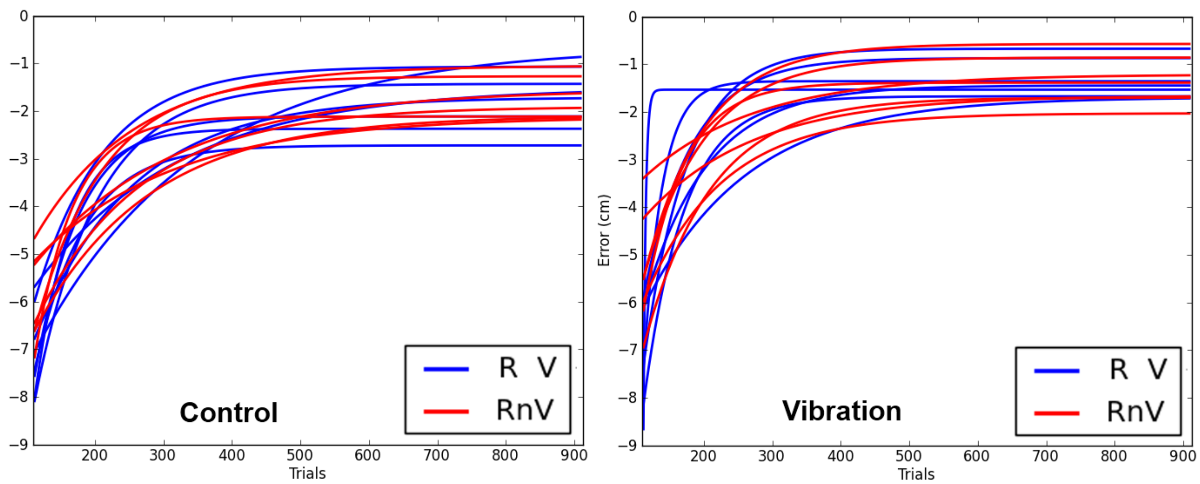

Figure 42: Comparison between the exponential regressions of RV and RnV trials.

In the control group, there is no significant difference between the parameters of the RV and RnV exponential regressions. Differently in the vibration group, the time constant C of the RV curves is significantly smaller ($p<0.03$) from the C of the RnV curves, with a Cohen's effect size *d* equal to 1.01; there is no significant difference between the other two parameters.

4.3.1.3 nRnV catch-trials

Figure 43 depicts how the nRnV catch-trials' MPE changes along the learning phase. In this figure, the trial-by-trial mean is represented by the blue line, while the light blue area represents the standard deviation. For both groups, the difference between the average of the last five RV trials and the average of the first five RV trials of this phase is significantly smaller than 0 ($p < 0.001$). Hence, the nRnV catch-trials' performance significantly ***worsened*** during the learning phase.

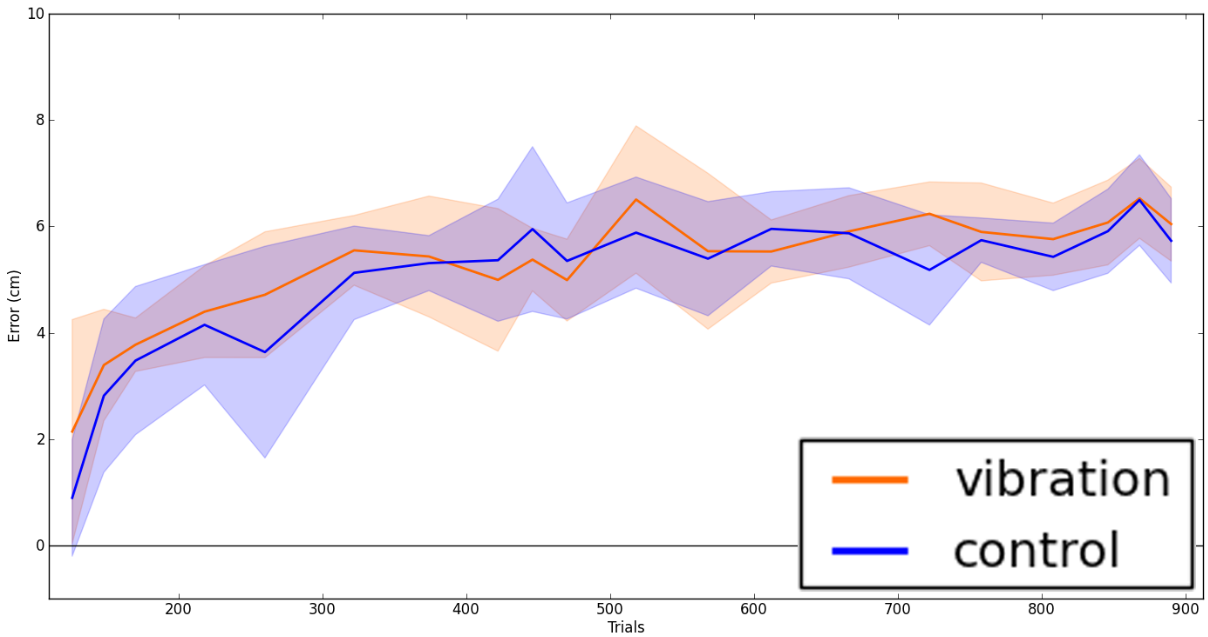

Figure 43: nRnV catch-trials' Maximum Perpendicular Error (MPE) of each group in the learning phase. The light colored areas are the standard deviations.

Similarly to the previous image, Figure 44 illustrates how the nRnV catch-trials' ET changes along the learning phase. For both groups, there is no significant difference between the average of the last five nRnV trials and the average of the first five nRnV trials of this phase. Hence, the RnV catch-trials' Execution Time did not significantly changed along this phase.

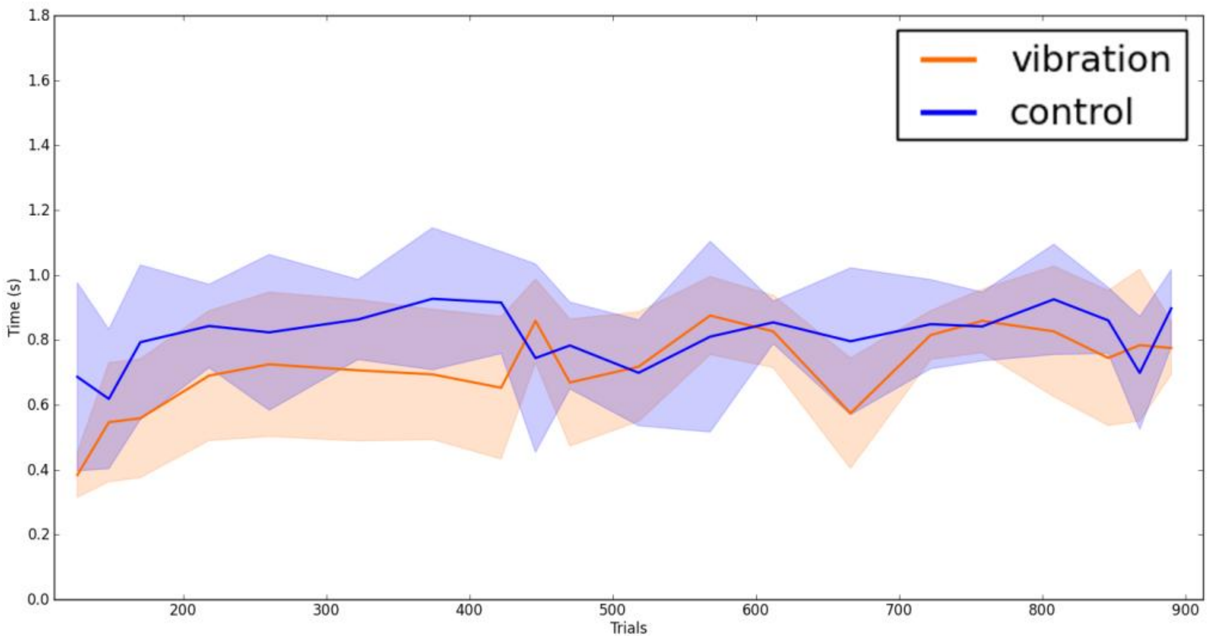

Figure 44: nRnV catch-trials' Execution Time (ET) of each group in the learning phase. The light colored areas are the standard deviations.

4.3.1.4 Performance plateau

The exponential model used to summarize the experimental data assumes the presence of a plateau during the learning phase. This plateau is the interval at the end of the learning curve where there is no more significant learning. To identify this plateau, an application was written that finds the maximum trial interval where each group did not significantly improve their performance. This application identified for both groups the maximum interval which terminates at the end of the learning phase, and where the average of the first ten trials is not significantly different from the average of the last ten trials (i.e. the last ten trials of the learning phase).

The beginning of the Maximum Perpendicular Error's plateau starts at trial number 320 in the vibration group (i.e. the ten consecutive RV trials starting with trial number 320 are not significantly different from the last ten RV trials of the learning phase), while it starts with the trial number 584 in the control group (Figure 45). According to this criterion, the vibration group reaches its performance plateau significantly earlier than the control group.

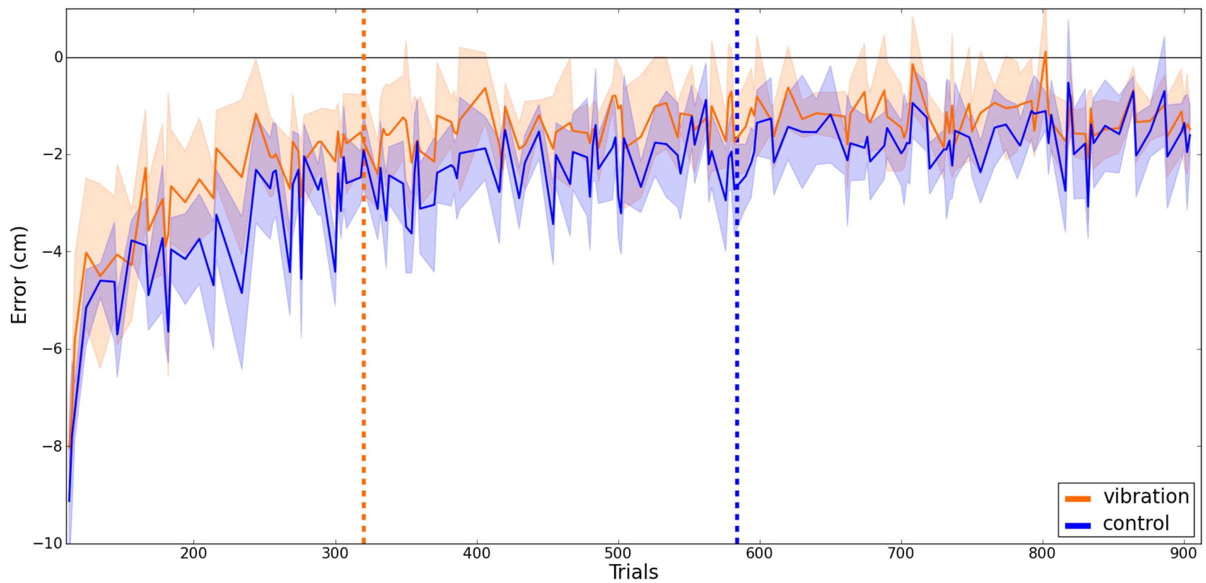

Figure 45: Trial-by-trial average of the RV trials' MPE. The light colored areas represent the standard deviations. The vertical dotted lines represent the beginning of the plateau where there is no more a significant improvement of the performance.

Similarly, the Initial Direction of Movement's plateau starts at the trial number 338 in the vibration group and at the trial number 432 for the control group. In contrast, the Execution Time's plateau starts at the trial number 338 in the vibration group and at the trial number 292 for the control group.

Hence, it is possible to say that the two features that express a displacement error reach earlier the plateau in the vibration group, while the feature that expresses the execution time reaches the plateau earlier in the control group.

4.3.2 Performance between groups

4.3.2.1 RV trials

Figure 46 depicts the exponential regression of each subject's MPE during the RV trials. The dominant time constant C of the vibration group is significantly less than the C of the control group ($p<0.05$), with $\mu_{C,vibr} = 65.9753, \sigma_{C,vibr} = 43.4891$, $\mu_{C,ctrl} = 121.0361$, and $\sigma_{C,ctrl} = 68.0473$. The Cohen's effect size *d* between the parameter C of the two populations is equal to 0. 0.9642. Instead, there is no significant difference between the B of the two groups, with $\mu_{B,vibr} = -6.0486, \sigma_{B,vibr} = 1.2656$, $\mu_{B,ctrl} = -5.3820$, and $\sigma_{B,ctrl} = 0.8394$. Finally, there is no significant difference also for the parameter A, with $\mu_{A,vibr} = -1.2571, \sigma_{A,vibr} = 0.4124$, $\mu_{A,ctrl} = -1.6999$, and $\sigma_{A,ctrl} = 0.6827$. The average R^2 of each regression is equal to 0.5520 with a standard deviation equal to 0.1006.

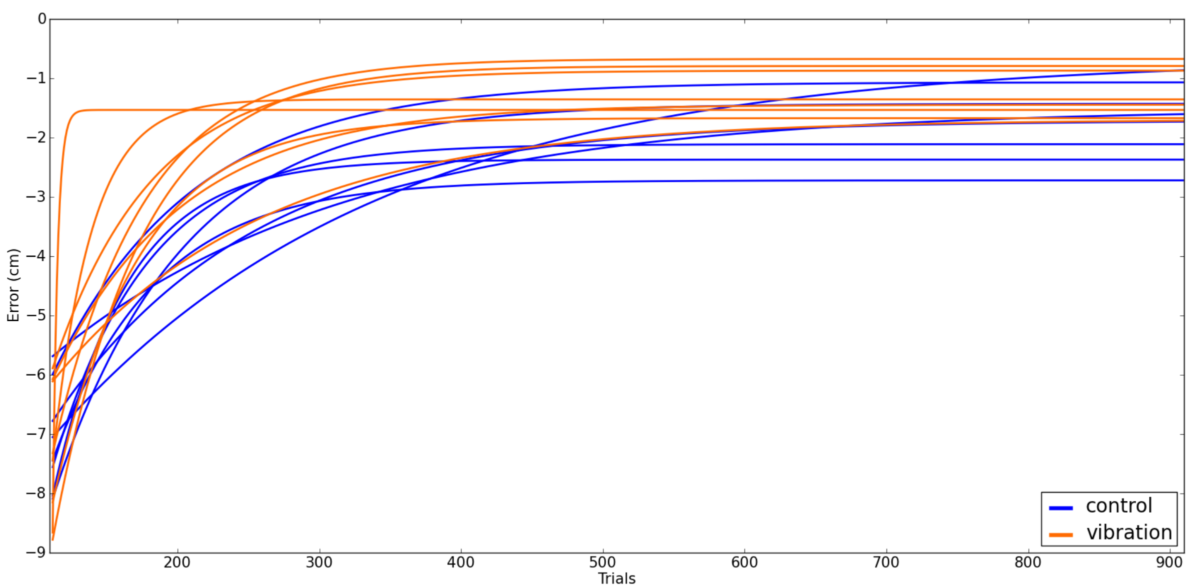

Figure 46: Exponential regression of the MPE's data of each subject's RV trials.

A Levene's test was performed on the three variables A, B and C to check the homogeneity of variance between the two groups. For all three variables, there is no significant difference between the variance of the two groups. Hence, the assumption of homoscedasticity was met.

4.3.2.2 RnV catch-trials

Figure 46 depicts the exponential regression of each subject's MPE during the RnV trials. The dominant time constant C of the vibration group is less than the C of the control group with a marginal statistic significance (p<0.1), with $\mu_{C,vibr} = 106.7406$, $\sigma_{C,vibr} = 36.9675$, $\mu_{C,ctrl} = 147.4871$, and $\sigma_{C,ctrl} = 54.3857$. The Cohen's effect size d between the parameter C of the two populations is equal to 0.8762. Instead, there is no significant difference between the B of the two groups, with $\mu_{B,vibr} = -4.2945$, $\sigma_{B,vibr} = 1.3322$, $\mu_{B,ctrl} = -4.2499$, and $\sigma_{B,ctrl} = 0.8394$. Finally, there is no significant difference also for the parameter A, with $\mu_{A,vibr} = -1.2617$, $\sigma_{A,vibr} = 0.5297$, $\mu_{A,ctrl} = -1.7327$, and $\sigma_{A,ctrl} = 0.4436$. The average R^2 of each regression is equal to 0.4891 with a standard deviation of 0.1033.

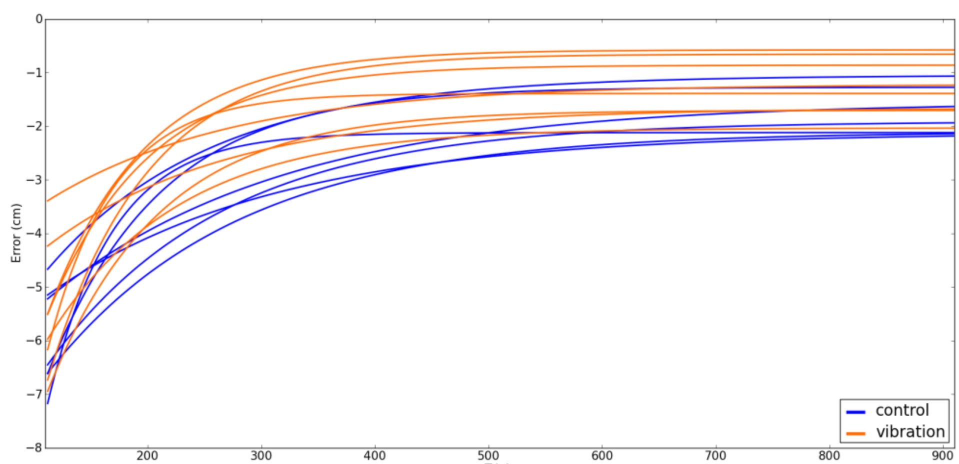

Figure 47: Exponential regression of the MPE's data of each subject's RnV catch-trials.

4.3.2.3 nRnV catch-trials

Figure 46 depicts the exponential regression of each subject's MPE during the nRnV trials. There is no significant difference between the three parameters A, B, and C, with $\mu_{C,vibr} = 133.5371$, $\sigma_{C,vibr} = 124.6698$, $\mu_{C,ctrl} = 123.3935$, and $\sigma_{C,ctrl} = 103.7678$, $\mu_{B,vibr} = -8.9138$, $\sigma_{B,vibr} = 7.5417$, $\mu_{B,ctrl} = -5.7174$, and $\sigma_{B,ctrl} = 2.6388$, $\mu_{A,vibr} = 6.1994$, $\sigma_{A,vibr} = 0.8738$, $\mu_{A,ctrl} = 5.8606$, and $\sigma_{A,ctrl} = 0.5986$. The average R^2 of each regression is equal to 0.6047 with a standard deviation of 0.2053.

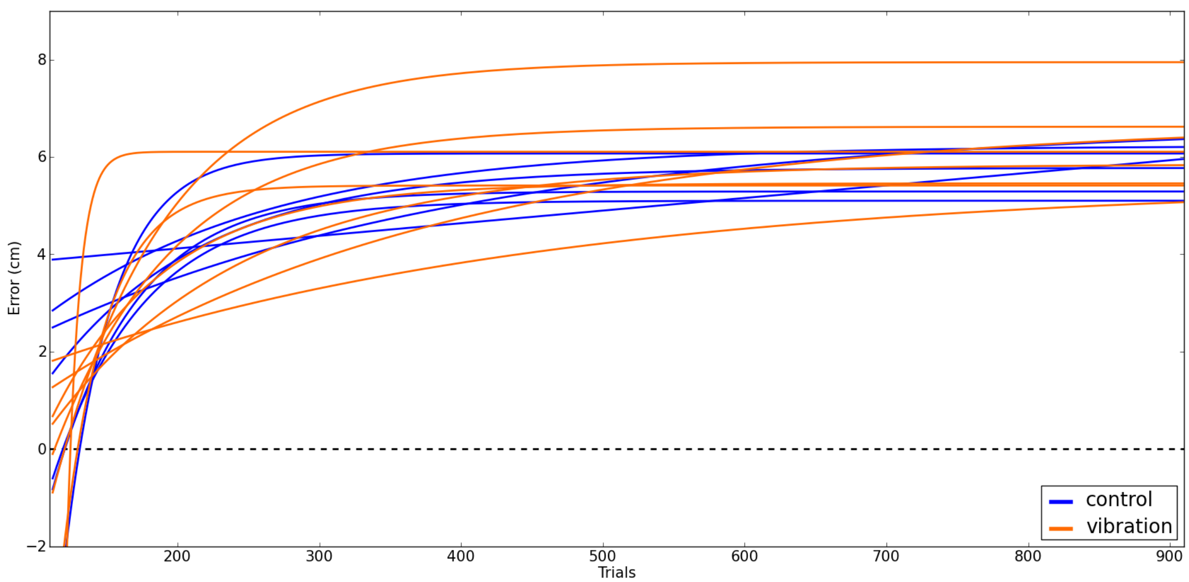

Figure 48: Exponential regression of the MPEs of each subject's nRnV catch-trials.

4.3.3 Learning Index

Figure 49 shows the exponential regression of the learning index of each subject. The subjects of the control group are blue, while the subjects of the vibration group are orange. The curves of the vibration group tends to be higher than the others, however there is no significant difference between the parameters of these curves.

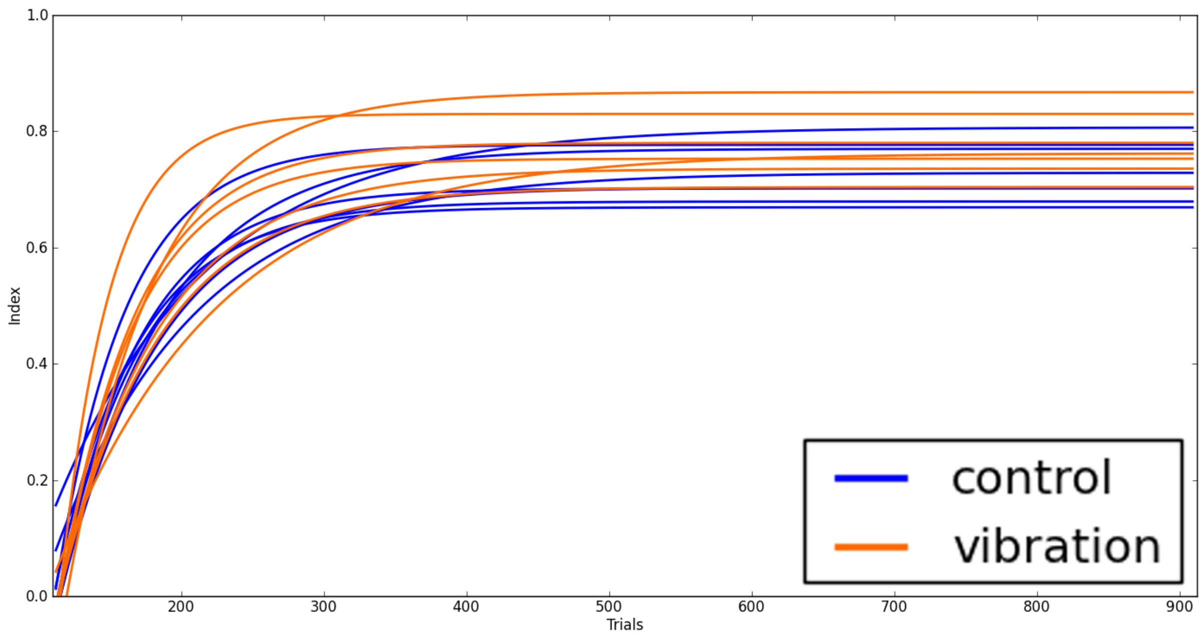

Figure 49: Exponential regression of each subject's learning index.

4.4 GENERALIZATION

The analysis of the generalization phase takes into consideration two aspects. First an analysis to detect the presence of a discontinuity between the end of the learning phase and the beginning of the generalization phase was performed. Then, a test to observe if there is a significant improvement of the performance during this phase was performed.

Figure 50 shows the MPE's average of the last learning phase's block and of the generalization's block. For both control and vibration groups, there is no significant difference between the last ten trials of the learning phase and the first ten trials of the generalization phase. This analysis was performed for the Maximum Perpendicular Error, the Execution Time and the Initial Direction of Movement.

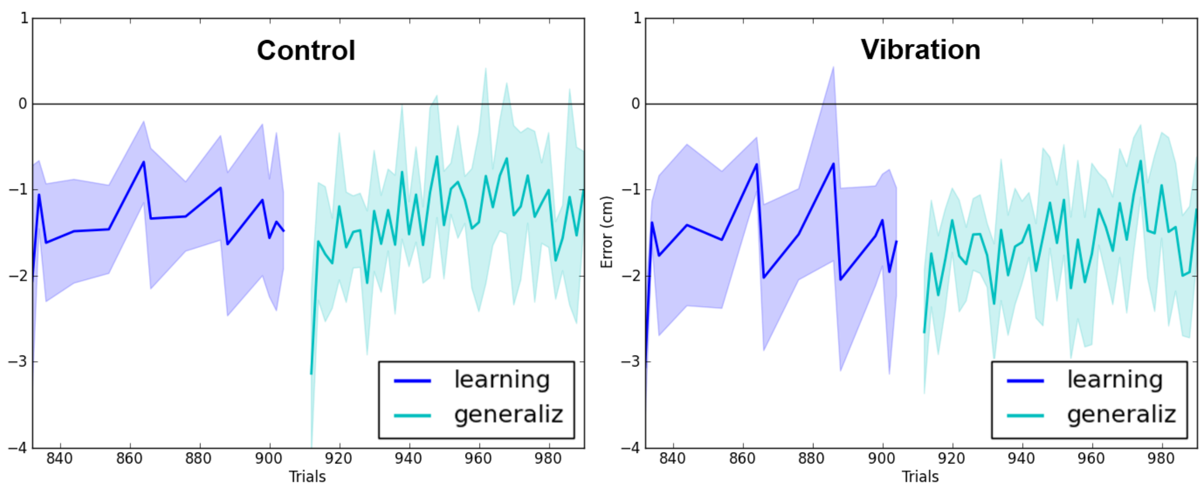

Figure 50: Trial-by-trial average of the Maximum Perpendicular Error at the end of the learning phase and at the beginning of the generalization phase. The light colored area represents the standard deviation.

Moreover, there is no significant difference between the beginning and the end of the generalization phase, for both groups and for all the features. This means that the performance remains unchanged in both groups for the entire duration of the generalization phase.

4.5 WASHOUT

Figure 51 shows the trial-by-trial average of the MPE error in both the baseline phase (Figure 51a) and the washout phase (Figure 51b).

MPE, ET and IDE are significantly higher in both groups during the first ten trials of the washout than during the last ten trials of the baseline ($p<0.01$). This indicates that the performance of the unperturbed task significantly worsens after the learning and generalization phases.

MPE, ET and IDE are significantly lower in both groups during the last ten trials of the washout than during the first ten trials of the same phase ($p<0.01$). This means that the performance improves during the washout phase.

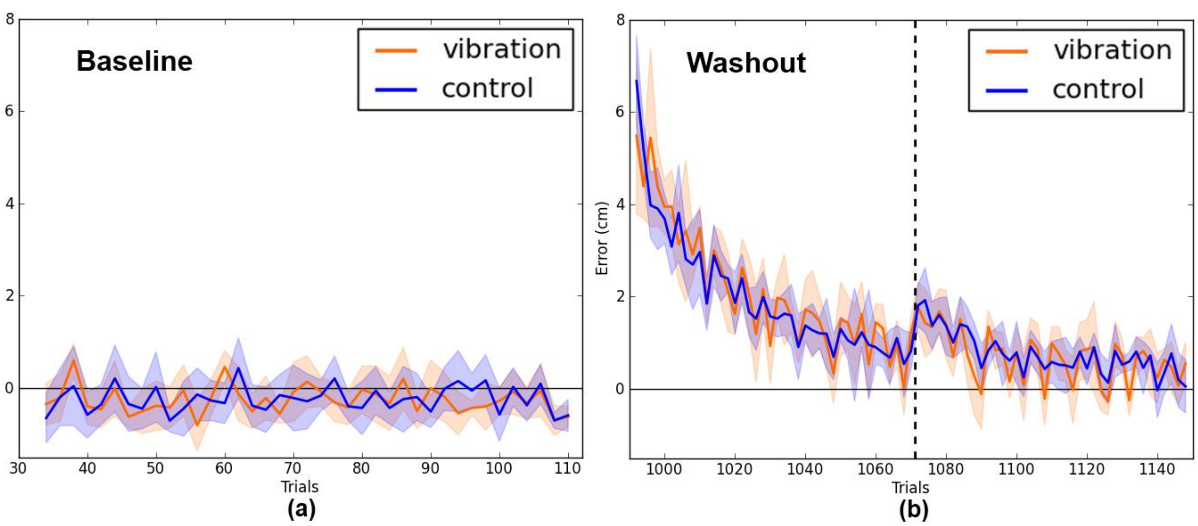

Figure 51: Mean MPS of both groups during (a) the baseline phase and (b) the washout phase. The light colored areas represent the standard deviation. The vertical dotted line in (b) represents a 40 seconds rest that divides the washout phases into two blocks.

There is no significant difference between the values of MPE, ET and IDE during the last ten trials of the baseline and the ones during the last ten trials of the washout. This means that at the end of the washout phase the performance went back to the pre-learning phase levels.

One last observation is about the 40 seconds rest that divides the washout phase into two blocks. This rest is depicted in Figure 51b by a vertical dotted line. In both groups, MPE and IDE are significantly higher during the first ten trials before the rest than during the last ten trials after the rest ($p<0.01$). This indicates that the performance is worst after the rest.

CHAPTER 5:

DISCUSSION

In this study, a reach-and-stop task was developed where the subjects had to adapt to a 60 degrees rotation of the visual field. The subjects were divided into two groups: the control group and the vibration group, which received the same feedbacks of the control group plus a vibrotactile feedback of the error. The primary objective of this research is to investigate if it is possible to provide a vibrotactile feedback to enhance the process of motor adaptation.

To evaluate the performance of each subject, an indicator of the time required to reach the targets (i.e. Execution Time) and three indicators of spatial displacement (i.e. Maximum Perpendicular Error, Initial Direction of Movement and Learning Index) were used. The spatial displacement indicators were more suitable to evaluate the performance because the experiment did not impose strict constraints on the execution time. The most appropriate indicator between the spatial displacement ones is the Maximum Perpendicular Error, because the other two indicators rely too much on the few nRnV catch-trials of the learning phase. In this Chapter the term error refers to the Maximum Perpendicular Error, if it is not specified otherwise.

5.1 THE SUBJECTS ADAPT TO THE VISUAL DISTORTION

The unperturbed reach-and-stop task can be easily performed by subjects of both groups. In fact, the average error of the baseline phase is not significantly different in the two groups, and it is between 2 and 3 millimeters. In some studies [85,87], the average value of the baseline is considered as a subject-dependent bias. In these studies, all the measurements of the following phases are adjusted for that bias, and their values become relative to the measurements of the baseline phase. However, for this study the values of the each phase are absolute, not relative. This decision was taken because it is not possible to know if the performance of the subjects was converging to an asymptote with a slope that cannot be perceived in the few trials of the baseline.

The error increased about 35 times (from 0.2 cm to 7-8 cm) when the visual distortion was introduced. This increase is not surprising, because the perturbation made the task confusing to the subjects. Hence, the performance during the very first few trials can be considered as the baseline of the perturbed task. In fact, the perturbation was applied without warnings, and the subjects cannot predict it.

It is interesting that there is no significant difference between the performances of the vibration group and the control group at the beginning of the learning phase. If we consider the exponential regression of the vibration group, there is no significant difference between the initial error of the RV and RnV trials. These two observations suggest that the vibrotactile feedback did not have an immediate effect on the performance. In other words, the subjects did not instinctively know how to use the vibration to detect increasing or decreasing error. This suggests that the subjects did not suffer significant startle reactions that could hamper performance. Moreover, the vibrotactile feedback is provided for the first time to the subjects at the beginning of the learning phase. Hence, it takes sometime before that the subjects can successfully apply the information from the vibrotactile feedback to counter the perturbation.

The error of the RV trials significantly decreased along the learning phase, and it reached a horizontal asymptote (called *learning plateau*) after some hundreds of repetitions. This implies that the subjects are able to compensate a constant 60 degrees rotation of the visual field. This result is not surprising, and it confirms the results of other studies [69,8,7,10,9]. However, it is important to point out that there is a significant difference between the error at the end of the learning curve and the error at the end of the baseline. The learning plateau leads to a residual error of about 1 cm in both groups, while in the baseline there was a residual error of about 0.2 cm. This means that the subjects were able to adapt to the visual distortion, but they were not able to completely compensate it. It is not possible to know if this phenomenon is due to the inability of the subjects to detect the error or to the motor system to correct for the detected error.

A remarkable stimulus for reflections comes from the questions asked to each subject after the end of the experiment. In fact, four subjects out of sixteen (one from the vibration group and three from the control group) did not understand that the increase of the error during the learning phase was caused by a visual rotation. However, they managed to decrease the error. These subjects barely noticed that, at the end of the learning phase, they were moving their hands in a different direction to reach the targets. The subjects that understood the presence of a rotation were not able to identify correctly the magnitude of the distortion, and all of them underestimated it with a value from 30 to 40 degrees. These observations raise interesting questions about the role of unconscious learning in motor adaptation. In fact, the subjects who did not realize the type of perturbation had a performance not significantly different from the others. However, this experiment was not designed to answer such a question, and it remains a simple speculation.

5.2 THE SUBJECTS CREATE AN INTERNAL MODEL

The data from the learning phase's trials shows us that the subjects of both groups were able to adapt to the visual rotation. However, as previously described in Chapter 2, the increase in performance by itself does not guarantee the creation of an internal model because this is not the only way for the subjects to compensate the visual distortion. To reach the conclusion that subjects are creating an internal model, it is necessary to analyze also the nRnV catch-trials and the washout phase.

The beginning of the washout phase shows a significant aftereffect which indicates a durable change in the controller used to perform the task. This aftereffect is characterized by an error significantly different from the error found in the baseline phase. Moreover, the sign of this aftereffect is opposite to the error during the learning phase.

This aftereffect indicates that the exposure to the visual distortion changed how the subjects executed the reach-and-stop task. This change is believed due to the adaptation of the internal model to the perturbation of the task, and is consistent with the hypothesis that subjects adapted to the distortion by using an internal model that approximate the novel dynamics of the environment. This phenomenon is consistent with previous studies on motor adaptation [6,20,87,19].

The error of the nRnV catch-trials is extremely useful to understand how the internal model is built during the learning phase. These catch-trials have neither vibration nor visual distortion, and the subjects cannot predict their appearance. Hence, the internal model produces the same motor output on RV trials and on nRnV catch-trials. We see in Figure 37 that the error in the catch-trials grew with practice during the learning phase. The learning index shows that most of the changes in the internal model took place in the early stages of the learning phase, in agreement with the presence of the learning plateau.

5.3 THE INTERNAL MODEL IS NOT TARGET-SPECIFIC

The generalization phase gives some insight on the robustness of the internal model. In fact, it is interesting to see how general the internal model appears to be. In particular, this phase of the experiment is used to find out if the subjects learned only a specific path that their hand had to follow, or if they learned a more general model that permits them to predict the effect of the distortion along a generic path.

In the experiment described in this document, the subjects were able to generalize the internal model of the visual distortion to novel trajectories. In fact, there is no significant difference between the error at the end of the learning phase and the error at the beginning of the generalization phase. Moreover, there is no significant improvement of performance during the generalization phase. This suggests that changing the trajectories did not help the subjects to get over the learning plateau.

Finally, it is important to point out that the generalization tested in this experiment helped to understand the trajectory-independency of the internal model. It would have been interesting to investigate also the rotation-independency (i.e. is the model valid also for other degrees of rotation?) and the retention (i.e. are the subjects able to remember over time what they learned?) of the model. However, these additional experiments were not performed because it does not help to answer the main question of this research and it would necessitate the addition of other experimental blocks and sessions to the protocol.

5.4 THE VIBROTACTILE FEEDBACK IS AN IMPORTANT CUE

The RnV catch-trials are extremely useful to understand how much the subjects of the vibration group rely on the vibrotactile feedback. In fact, in the vibration group these catch-trials did not provide this cue, while in the control group they are completely equivalent to the RV trials.

According with 4.3.1.2, in the control group there is no significant difference between the exponential regressions of RV trials and the ones of RnV catch-trials. However, in the vibration group the dominant time constant C of the RV trials is significantly smaller than those of the RnV catch-trials, while there is no significant difference between the other parameters. In other words, the beginnings and the ends of these curves are not significantly different, but in between the RV curves presents less error than the RnV curves.

This implies that the subjects of the vibration group, initially, did not rely on the vibrotactile feedback. However, after few trials, the subjects started relying more and more on the vibrotactile feedback. Yet, after reaching a peak, this dependence disappears the closer the subjects get to the learning plateau.

It is important to consider that the subjects had never been exposed to the vibrotactile feedback before the beginning of the learning phase. A possible interpretation of this phenomenon is that the subjects needs time to understand the meaning of the information transmitted by the vibrotactile feedback. At the beginning of the experiments the subjects were instructed to associate the vibration with the error made. However, some time could be required to associate the amplitude of the vibration with the magnitude of the error.

It is extremely interesting that the vibrotactile feedback did not introduce a significant difference in the error at the beginning of the learning phase. In fact, this shows that vibration neither reduced nor increased the error, and for this reason it is possible to exclude the presence of startle reactions.

However, after few trials the subjects learned to use to the vibrotactile feedback, and relying more on this information. In fact, the error of the RV trials became smaller than the error of the RnV catch-trials. This difference disappeared at the end of the learning curve because both RV trails and RnV catch-trials reached the same learning plateau. An explanation of this phenomenon is that as the error decreased so did the vibration, until the vibrotactile feedback reached a so small level of amplitude that it was ignored by the subjects. At the end of the learning curve, the subject clearly did not rely any more on the vibrotactile feedback. Evidence to this phenomenon comes from the performance during the generalization phase, where the vibrotactile feedback was not provided. In fact, the performance of this phase is not significantly different from the performance at the end of the previous phase. Hence, the subjects relied on the vibrotactile feedback only while they were learning to compensate the distortion, and after they become independent from it.

5.5 VIBRATION ENHANCE LEARNING

As previously described in Section 4.3.2.1, the parameters of the exponential regressions are extremely helpful to compare the performance of the two groups. It is possible to say that ***in the vibration groups the error decreased two times faster than in the control group***, and that there is no significant difference between the initial error and the asymptotic error of the two groups.

As previously stated, the decrease of performance by itself is not sufficient to warrant a judgment about the learning process. Moreover, Section 4.3.3 shows that there is no significant difference between the learning index of the two groups. However, it is important to keep in mind that the learning index relies mainly on the values of the nRnV catch-trials, which are particularly sensitive to noise due to the small number of samples. The purpose of these trials is to show the growth of the internal model, and not to quantify this growth. In fact, as previously described in Section 3.2, the presence of a high number of catch-trials alters the task and hampers the performance.

The faster reduction in performance, the generation of an internal model, and the target-independence of the internal model give us enough evidence to conclude that the use of a vibrotactile feedback enhances motor adaptation to a 60 degrees rotation of the visual field.

5.6 THERE IS OBLIVION AFTER THE RESTS

One last observation is about how performance is influenced by rests. Figure 51b depicts a significant increment of the error after the rest between the two blocks of the washout phase. The washout is particularly indicated to observe this effect thanks to the steep decrease of the error and the trivial nature of the task. In the learning phase it is not possible to observe this phenomenon, probably due to the high level of noise and variance that is present in this phase.

This observation confirms that it is necessary to reject the trial's data which follows rests and catch-trials. The rejection of this data is useful to reduce the noise and the variance of the data.

CHAPTER 6:

CONCLUSIONS

In this document, a new training strategy for motor adaptation was evaluated: a vibrotactile feedback which encodes the magnitude of the error made by the subjects. The results of this experiment suggest that such a vibrotactile feedback has the potential to increase the speed of adaptation.

In this experiment, the subjects had to adapt to a 60 degrees rotation of the visual field in a reach-and-stop task for the upper limbs. The subjects of both the vibration group and the control group managed to compensate this perturbation by updating the internal model of the environment dynamics. Despite some subjects were not able to explain the nature of the perturbation, all the subjects were able to apply the updated internal model to a generalized task with novel targets' positions.

The time required by the vibration group to compensate the visual rotation was significantly shorter than the one required by the control group. The learning curve was regressed to an exponential model, and the dominant time constant of the vibration group was almost two times smaller than the one of the control group. This phenomenon was confirmed by the learning plateau. In fact, both the vibration group and the control group reached the same learning plateau, but the vibration group reached this plateau significantly earlier than the control group.

The result of this experiment suggests that a vibrotactile feedback can be successfully used to enhance motor adaptation. Three arguments are particularly interesting for future works. First of all, the vibrotactile feedback should be properly compared with other Error Augmentation techniques. Then, it is interesting to investigate if the beneficial effect of vibration is present with other kinds of perturbations. Finally, new ways to encode the vibrotactile feedback to maximize its beneficial effect should be studied.

Despite the protocol used in this experiment was different by the ones used in the literature, it is possible to perform a preliminary comparison between the results of this experiment and the results of other studies. In fact, in [7,8,69,10,38] the Error Augmentation (EA) groups presented a time constant which was significantly smaller than the one of correspondent control groups. The groups with Force EA presented also an increased amount of learning. However, it is important to notice that Force EA, differently from Visual EA and vibration, changes the dynamics of the environment and causes a higher initial error.

The vibrotactile feedback presents some interesting advantages compared to Visual and Force Error Augmentation:

- **devices requirements:** if the only error-encoded feedback provided to the users is a vibrotactile feedback, then it is no longer necessary to use the complex virtual reality system required by both Visual EA and Force EA. In fact, it could be possible to design a system composed by a vibrotactile actuator and a tracking system to detect the position of the user’s hand and of the targets. The targets could become physical targets moved by either a robotic device or a therapist.

- **risk of instability:** the main issue of Force EA is that this technique alters the task’s dynamics and introduce an high risk of instability. For this reason, there are strong limitations to gain used encode the error into a force [5]. Moreover, a physical increase (and not only a virtual one) of the error done by the user could become dangerous in some applications (e.g. driving, rehabilitation of severe impaired patients). The vibrotactile feedback, similarly to Visual EA, does not have this problem because it does not change the task's dynamics.

- **rejection:** studies done on Visual EA [7,8] shows that there is no significant enhancement if an high gain is used to encode the error into a visual displacement. A possible explanation of this phenomenon is that high gains deforms too much the trajectories, and the users rejects this information because they do not recognize in this altered trajectory the movement that they are doing. In fact, the subjects are used to perceive both the visual feedback of their movements and the proprioceptive perception of their limbs' position. Most likely, the vibrotactile feedback does not have this issue because there are no predefined relationships between the amplitude of the vibration and the movement done with the hand. The users create this relationship at the beginning of the learning phase by associating the error that they are doing with the magnitude of the vibration.

The objective of this experiment was to perform an explorative analysis to understand if vibrotactile feedbacks could be used to enhance motor adaptation. To avoid the introduction in the experiment of not necessary variables, the encoding of the vibrotactile feedback was kept as simple as possible. Future works could analyze new ways to provide this feedback to maximize its beneficial effect on motor adaptation. The following are some examples of possible experiments:

- **encoding of direction:** in this experiment the vibration is proportional only to the magnitude of the error. However, it is possible to encode also the direction of the error using multiple vibrotactile actuators.

- **different positions of vibrotactile display:** in this experiment the vibrotactile actuator is located on the index of the dominant harm. It is interesting to analyze if it is possible to obtain similar results positioning the actuator in other positions on the subjects' body. In this way, it could be possible to stimulate more accessible or more sensible areas. For example, a hemi-paretic stroke survivor could have problems to perceive vibrations in the arm that needs to be rehabilitated.

- **different encoding technique:** in this experiment the vibration was linearly proportional to the magnitude of the error. However, this is not the only way to encode it. For example, in [11] the gain used to encode the error of a tele-operation task into a vibrotactile feedback was increased during the experiment to break the learning plateau. The result of this study suggests that it is possible to dynamically change the proportion between error and vibration to obtain more precise trajectories. Another way to encode the error could keep in consideration that, according to [88], the relationship between the amplitude of the vibration and the subjective perception of this vibration is not linear. In other words, if vibration amplitude of 100 μm in a subject is equivalent to a subjective perception of 1, then a vibration amplitude of 200 μm is not equivalent to a subjective perception of 2. According to Stevens' Power Law this relationship is exponential, and the encoding of the error could keep in consideration this aspect.

- **pseudo-random vibrotactile feedback:** it would be interesting to add a group exposed to a pseudo-random vibrotactile feedback. This feedback would have the same distribution of vibration intensity and the same frequency spectrum as in the experiments for the vibration group. If performance of this group was similar to the vibration group, then one might infer that motor adaptation process is enhanced by adding an alerting feedback. In other words, this could show that we need not add a vibrotactile feedback proportional to the error to enhance learning, but merely the addition of a novel feedback which increase the subjects' level of attention. However, if this group showed a worse performance, then it is clear that the enhancement is correlated with the addition of a feedback proportional to the error.

Thanks to the flexibility of the device used to perform the experiment described in this document, all the examples of future experiments described in this Chapter can be easily obtained with small modifications of the current experiment.

CITED LITERATURE

1. EAI website: http://www.eaiinfo.com/Tactor%20Products.htm

2. Akamatsu, M., MacKenzie, S., and Hasbrouc, T. "A Comparison of Tactile, Auditory, and Visual Feedback in a Pointing Task Using a Mouse-Type Device," *Ergonomics* Vol. 38, No. 4, 1995, pp. 816-827.

3. Alahakone, A., and Arosha Senanayake, A. "Vibrotactile feedback systems: Current trends in rehabilitation, sports and information display," *IEEEASME Conference*, 2009, pp. 1148-1153.

4. Alegria, J. "Sequential effects of catch-trials on choice reaction time," *Acta Psychologica* Vol. 42, No. 1, 1978, pp. 1–6.

5. Barber, R., and Lucas, H. "System Response Time, Operator Productivity, and Job Satisfaction," *ACM* Vol. 26, No. 11, 1983, pp. 972-986.

6. Bhushan, N., and Shadmehr, R. "Computational nature of human adaptive control during learning of reaching movements in force fields," *Biol Cybern* Vol. 81, No. 1, 1999, pp. 39-60.

7. Brown, L., Brewster, S., and Purchase, H. "A First Investigation into the Effectiveness of Tactons," *First Joint Eurohaptics Conference and Symposium on Haptic Interfaces for Virtual Environment and Teleoperator Systems World Haptics Conference*, 2005, pp. 167-176.

8. Burgar, C. G., Lum, P. S., Shor, P. C., and Machiel Van der Loos, H. F. "Development of robots for rehabilitation therapy: the Palo Alto VA/Stanford experience," *J Rehabil Res Dev* Vol. 37, No. 6, 2000, pp. 663-73.

9. Burke, J., Prewett, M., Gray, A., Yang, L., Stilson, F., Coovert, M., Elliott, L., and Redden, E. "Comparing the effects of visual-auditory and visual-tactile feedback on user performance: a meta-analysis," *ACM*, 2006, p. 108.

CITED LITERATURE (Continue)

10. Casadio, M., Morasso, P., Sanguineti, V., and Giannoni, P. "Minimally assistive robot training for proprioception enhancement," *Exp Brain Res* Vol. 194, No. 2, 2009, pp. 219-31.

11. Celik, O., Powell, D., and O'Malley, M. "Impact of visual error augmentation methods on task performance and motor adaptation," *Mechanical Engineering*, 2009, pp. 793-798.

12. Cholewiak, R., and Wollowitz, M. "The design of vibrotactile transducers," *Tactile Aids for the Hearing Impaired*. I. Summers, ed, Whurr Publishers Ltd, London, 1992.

13. Coote, S., and Stokes, E. "Robot mediated therapy: Attitudes of patients and therapists towards the first prototype of the GENTLE/S system," *Technology and Disability* Vol. 15, No. 1, 2003, pp. 27-34.

14. Criscimagna-Hemminger, S. E., Donchin, O., Gazzaniga, M. S., and Shadmehr, R. "Learned dynamics of reaching movements generalize from dominant to nondominant arm," *J Neurophysiol* Vol. 89, No. 1, 2003, pp. 168-76.

15. Cruz-Neira, C., Sandin, D., DeFanti, T., and Kenyon, R. "The CAVE: audio visual experience automatic virtual environment," *ACM* Vol. 35, No. 6, 1992, pp. 64-72.

16. Czernuszenko, M., Pape, D., Sandin, D., DeFanti, T., Dawe, G., and Brown, M. "The ImmersaDesk and Infinity Wall projection-based virtual reality displays," *ACM SIGGRAPH* Vol. 31, No. 2, 1997, pp. 46-49.

17. Davidson, P. R., and Wolpert, D. M. "Motor learning and prediction in a variable environment," *Curr Opin Neurobiol* Vol. 13, No. 2, 2003, pp. 232-7.

18. Dvorkin, A., Rymer, W., Harvey, R., Bogey, R., and Patton, J. "Assessment and monitoring of recovery of spatial neglect within a Virtual Environment," *Virtual rehabilitation*, 2008, pp. 88-92.

19. Dvorkin, A., Zollman, F., Beck, K., Larson, E., and Patton, J. "A virtual environment-based paradigm for improving attention in TBI," *ICORR* 2009, pp. 962-965.

CITED LITERATURE (Continue)

20. Emken, J., Benitez, R., Sideris, A., Bobrow, J., and Reinkensmeyer, D. "Motor adaptation as a greedy optimization of error and effort," *Journal of Neurophysiology* Vol. 97, No. 6, 2007, pp. 3997-4006.

21. Emken, J. L., Benitez, R., and Reinkensmeyer, D. J. "Human-robot cooperative movement training: learning a novel sensory motor transformation during walking with robotic assistance-as-needed," *J Neuroeng Rehabil* Vol. 4, 2007, p. 8.

22. Emken, J. L., and Reinkensmeyer, D. J. "Robot-enhanced motor learning: accelerating internal model formation during locomotion by transient dynamic amplification," *IEEE Trans Neural Syst Rehabil Eng* Vol. 13, No. 1, 2005, pp. 33-9.

23. Felix, C., Patton, J., and Mussa-Ivaldi, F. "Negative viscosity can enhance learning of internal dynamics," *IEEE Trans Neural Syst Rehabil Eng* Vol. 13, No. 1, 2009, pp. 33-39.

24. Franklin, D., So, U., and Kawato, M. "Visual Feedback Is Not Necessary for the Learning of novel dynamics," *PLoS ONE* Vol. 2, No. 12, 2007, p. 14.

25. Gallace, A., Tan, H., and Spence, C. "The body surface as a communication system: The state of the art after 50 years," *Presence* Vol. 16, No. 6, 2007, pp. 655-676.

26. Garrison, K. A., Winstein, C. J., and Aziz-Zadeh, L. "The mirror neuron system: a neural substrate for methods in stroke rehabilitation," *Neurorehabil Neural Repair* Vol. 24, No. 5, 2010, pp. 404-12.

27. Gillespie, B., O'Modhrain, S., Tang, P., Pham, C., and Zaretsky, D. "The virtual teacher," *ASME DSCD* Vol. 27, No. 96, 1998, pp. 935-954.

28. Harwin, W., and Hillman, M. "Introduction to special issue : Robotic assistance in neuro-motor therapy," *IEEE Transactions* Vol. 21, 2003.

CITED LITERATURE (Continue)

29. Harwin, W., Loureiro, R., Amirabdollahian, F., Taylor, L., Johnson, G., Stokes, E., Coote, S., Topping, M., Collin, C., Tamparis, S., Kontoulis, J., Munih, M., Hawkins, P., and Driessen, B. "The GENTLES/S project: A new method of delivering neuro-rehabilitation," *Journal of rehabilitation* Vol. 10, 2001.

30. Hatfield, B., Wyatt, W., and Shea, J. "Effect of auditory feedback on movement time in a fitts task," *J Motor Behav.* Vol. 42, No. 5, 2010, pp. 289-293.

31. Holden, M. "Neurorehabilitation using "lerning by imitation" in virtual enviroments," *Usability Evaluation and Interface Design: Cognitive Engineering, Intelligent Agents and Virtual Reality*. 2001.

32. Johnson, A., Dan, S., Dawe, G., Defanti, T., Pape, D., Qiu, Z., Thongrong, S., and Plepys, D. "Developing the PARIS: Using the CAVE to Prototype a New VR Display," *Proceedings of IPT*, 2000, pp. 19–20.

33. Krebs, H., Hogan, N., Volpe, B., Aisen, M., Edelstein, L., and Diels, C. "Robot-aided Neuro-rehabilitation in Stroke: Three Year follow-up," *Journal of NeuroEngineering*, 1999.

34. Krebs, H. I., Hogan, N., Aisen, M. L., and Volpe, B. T. "Robot-aided neurorehabilitation," *IEEE Trans Rehabil Eng* Vol. 6, No. 1, 1998, pp. 75-87.

35. Krebs, H. I., Hogan, N., Volpe, B. T., Aisen, M. L., Edelstein, L., and Diels, C. "Overview of clinical trials with MIT-MANUS: a robot-aided neuro-rehabilitation facility," *Technol Health Care* Vol. 7, No. 6, 1999, pp. 419-23.

36. Kuhmann, W., Boucsein, W., Schaefer, F., and Alexander, J. "Experimental investigation of psychophysiological stress-reactions induced by different system response times in human-computer interaction," *Ergonomics* Vol. 30, No. 6, 1987, pp. 933-43.

37. Lambert, G. "A Comparative Study of System Response Time on Program Developer Productivity," *Time* Vol. 23, No. 1, 1984, pp. 36-43.

38. Langhorne, P., Coupar, F., and Pollock, A. "Motor recovery after stroke: a systematic review," *Lancet Neurol* Vol. 8, No. 8, 2009, pp. 741-54.

CITED LITERATURE (Continue)

39. Lederman, S. J., and Klatzky, R. L. "Haptic perception: a tutorial," *Atten Percept Psychophys* Vol. 71, No. 7, 2009, pp. 1439-59.

40. Liu, J., Cramer, S., and Reinkensmeyer, D. "Learning to perform a new movement with robotic assistance: comparison of haptic guidance and visual demostration," *J. NeuroEng. and Rehab.* Vol. 3, No. 3, 2006, p. 20.

41. Lum, P., Burgar, C., Shor, P., Majmundar, M., and Van der Loos, H. "Robot-assisted movement training compared with conventional therapy techniques for the rehabilitation of upper limb motor function following stroke," *A. Phys. Med. and Rehab* Vol. 83, No. 7, 2002, pp. 952-959.

42. Lum, P. S., Burgar, C. G., Kenney, D. E., and Van der Loos, H. F. "Quantification of force abnormalities during passive and active-assisted upper-limb reaching movements in post-stroke hemiparesis," *IEEE Trans Biomed Eng* Vol. 46, No. 6, 1999, pp. 652-62.

43. Marchal Crespo, L., and Reinkensmeyer, D. "Haptic guidance can enhance motor learning of a steering task," *J. Mot. Behav.* Vol. 40, No. 6, 2008, pp. 545-556.

44. Massimino, M. "Improved force perception through sensory substitution," *Control Engineering Practice* Vol. 3, No. 2, 1995, pp. 215-222.

45. Mussa-Ivaldi, F., and Patton, J. "Robots can teach people how to move their arm," *ICRAA Proceedings*, 2000, pp. 300-305.

46. Mussa-Ivaldi, F., and Patton, J. "Robotic Teaching by Exploiting the Nervous System's Adaptive Mechanisms," *Int Conf on Rehab Rob*, 2001, pp. 3-7.

47. Mussa-Ivaldi, F., and Patton, J. "Linear Combinations of Nonlinear Models for Predicting Human-Machine Interface Forces," *Biological Cybernetics* Vol. 86, No. 1, 2002, pp. 73-87.

48. Mussa-Ivaldi, F., Patton, J., and Rymer, W. "Altering Movement Patterns in Healthy and Brain-Injured Subjects Via Custom Designed Robotic Forces," *IEEE Eng Med Bio* Vol. 2, No. 2, 2001, pp. 1356-1359.

CITED LITERATURE (Continue)

49. O'Malley, M., Gupta, A., Gen, M., and Li, Y. "Shared control in haptic systems for performance enhancement and training," *J. Dyn. Syst. Meas. Control* Vol. 128, No. 1, 2006, p. 75.

50. Patton, J., Dawe, G., Scharver, C., Mussa-Ivaldi, F., and Kenyon, R. "Robotics and Virtual Reality: A Perfect Marriage for Motor Control Research and Rehabilitation," *RESNA* Vol. 18, No. 2, 2004, pp. 181-195.

51. Patton, J., and Mussa-Ivaldi, F. "Robot-assisted adaptive training: custom force fields for teaching movement patterns," *IEEE Trans Biomed Eng* Vol. 51, No. 4, 2003, pp. 636-646.

52. Patton, J., Stoycov, M., Kovic, M., and Mussa-Ivaldi, F. "Evaluation of robotic training forces that either enhance or reduce error in chronic hemiparetic stroke survivors," *Exp Brain Res* Vol. 168, No. 3, 2006, pp. 368-383.

53. Patton, J., Wei, Y., Scharver, C., Kenyon, R., and Scheidt, R. "Motivating Rehabilitation by Distorting Reality," *IEEE RASEMBS Proceedings*, 2006, pp. 869-874.

54. Reinkensmeyer, D., and Patton, J. "Can robots help the learning of skilled actions?," *Exercise and Sport Sciences Reviews* Vol. 37, No. 1, 2009, pp. 43-51.

55. Reinkensmeyer, D. J., Dewald, J. P., and Rymer, W. Z. "Guidance-based quantification of arm impairment following brain injury: a pilot study," *IEEE Trans Rehabil Eng* Vol. 7, No. 1, 1999, pp. 1-11.

56. Reinkensmeyer, D. J., Kahn, L. E., Averbuch, M., McKenna-Cole, A., Schmit, B. D., and Rymer, W. Z. "Understanding and treating arm movement impairment after chronic brain injury: progress with the ARM guide," *J Rehabil Res Dev* Vol. 37, No. 6, 2000, pp. 653-62.

57. Reinkensmeyer, D. J., Pang, C. T., Nessler, J. A., and Painter, C. C. "Web-based telerehabilitation for the upper extremity after stroke," *IEEE Trans Neural Syst Rehabil Eng* Vol. 10, No. 2, 2002, pp. 102-8.

CITED LITERATURE (Continue)

58. Reinkensmeyer, D. J., Schmit, B. D., and Rymer, W. Z. "Assessment of active and passive restraint during guided reaching after chronic brain injury," *Ann Biomed Eng* Vol. 27, No. 6, 1999, pp. 805-14.

59. Reinkensmeyer, D. J., Schmit, B. D., and Rymer, W. Z. "Mechatronic assessment of arm impairment after chronic brain injury," *Technol Health Care* Vol. 7, No. 6, 1999, pp. 431-5.

60. Rupert, A. H. "An instrumentation solution for reducing spatial disorientation mishaps," *IEEE Eng Med Biol Mag* Vol. 19, No. 2, 2000, pp. 71-80.

61. Scharver, C., Evenhouse, R., Johnson, A., and Leigh, J. "Pre-surgical Cranial Implant Design using the PARIS™ Prototype," *IEEE Virtual Reality*, 2004.

62. Scheidt, R. A., Conditt, M. A., Secco, E. L., and Mussa-Ivaldi, F. A. "Interaction of visual and proprioceptive feedback during adaptation of human reaching movements," *J Neurophysiol* Vol. 93, No. 6, 2005, pp. 3200-13.

63. Scheidt, R. A., Dingwell, J. B., and Mussa-Ivaldi, F. A. "Learning to move amid uncertainty," *J Neurophysiol* Vol. 86, No. 2, 2001, pp. 971-85.

64. Schmidt, and Wrisberg. "Motor Learning and Performance," *Human Kinetics* Vol. 2, 2004, p. 339.

65. Shadmehr, R., and Mussa-Ivaldi, F. A. "Adaptive representation of dynamics during learning of a motor task," *J Neurosci* Vol. 14, No. 5 Pt 2, 1994, pp. 3208-24.

66. Sharp, I., Huang, F. C., and Patton, J. L. "Visual error augmentation enhances learning in three dimensions," *Conf Proc IEEE Eng Med Biol Soc* Vol. 2010, 2010, pp. 5915-8.

67. Sheidt, R., Conditt, M., Secco, E., and Mussa-Ivaldi, F. "Interaction of Visual and Proprioceptive Feedback During Adaptation of Human Reaching Movements," *J Neurophysiol* Vol. 93, No. 6, 2005, pp. 3200-3213.

CITED LITERATURE (Continue)

68. Shimoga, K. "Finger force and touch feedback issues in dextrous telemanipulation," *IEEE IRSSE*, 1992, pp. 159-178.

69. Smith, M., and Shadmehr, R. "Intact Ability to Learn Internal Models of Arm Dynamics in Huntington's Disease but not Cerebellar Degeneration.," *J Neurophysiol* Vol. 93, No. 5, 2005, pp. 2809-2821.

70. Sung, C., and O'Malley, M. K. "Effect of progressive visual error amplification on human motor adaptation," *IEEE Int Conf Rehabil Robot* Vol. 2011, 2011, p. 5975399.

71. Teal, S., and Rudnicky, A. "A Performance Model of System Delay and User Strategy Selection," *SIGCHI Proceedings*, 1992, pp. 295-305.

72. Tsukada, K., and Yasumura, M. "ActiveBelt: Belt-Type Wearable Tactile Display for Directional Navigation," *UbiComp2004 Proceedings*, 2004, pp. 384-399.

73. Van Der Linden, J., Johnson, R., Bird, J., Rogers, Y., and Schoonderwaldt, E. "Buzzing to play: lessons learned from an in the wild study of real-time vibrotactile feedback," *Human Factors in Comp Sys*, 2011, pp. 533-542.

74. Van Erp, J., and Van Veen, H. "A Multipurpose Tactile Vest for Astronauts in the International Space Station," *Eurohaptics Proceedings*, 2003, pp. 405-408.

75. Van Erp, J., Van Veen, H., Jansen, C., and Dobbins, T. "Waypoint navigation with a vibrotactile waist belt," *ACM Transactions* Vol. 2, No. 2, 2005, pp. 106-117.

76. Vergaro, E. *Adaptive robot therapy to promote the recovery of motor functions in Stroke survivors and Multiple Sclerosis subjects*, 2010.

77. Vergaro, E., Squeri, V., Brichetto, G., Casadio, M., Morasso, P., Solaro, C., and Sanguineti, V. "Adaptive robot training for the treatment of incoordination in Multiple Sclerosis," *J Neuroeng Rehabil* Vol. 7, 2010, p. 37.

CITED LITERATURE (Continue)

78. Visell, Y. "Tactile sensory substitution: Models for enaction in HCI," *Interacting with Computers* Vol. 21, No. 1-2, 2009, pp. 38-53.

79. Volpe, B., Lo, A., and Guarino, P. "Robot-assisted therapy for long-term upper-limb impairment after stroke," *N Engl J Med* Vol. 362, No. 19, 2010, pp. 1772-1783.

80. Wei, Y., and Patton, J. "Force Field Training to Facilitate Learning Visual Distortions: A "Sensory Crossover" Experiment," *HAPTICS Proceedings*, 2004.

81. Wei, Y., and Patton, J. "A real time haptic graphic demostration of how error augmentation can enhance learning," *IEEE ICRA*, 2005, pp. 4406-4411.

82. Winstein, C. J., Pohl, P. S., and Lewthwaite, R. "Effects of physical guidance and knowledge of results on motor learning: support for the guidance hypothesis," *Res Q Exerc Sport* Vol. 65, No. 4, 1994, pp. 316-23.

83. Wolpert, D. M., Ghahramani, Z., and Flanagan, J. R. "Perspectives and problems in motor learning," *Trends Cogn Sci* Vol. 5, No. 11, 2001, pp. 487-494.

84. Wulf, G., Shea, C., and Lewthwaite, R. "Motor skill learning and performance: a review of influential factors," *Med Educ* Vol. 44, No. 1, 2010, pp. 75-84.

85. Zwislocki, J. *Sensory Neuroscience. Four Laws of Psychophysics*: Springer, 2009.

VITA

NAME:	Alberto Gnemmi
EDUCATION:	Bachelor of Science in Computer Engineering, Politecnico di Milano, 2009.
	Master of Science in Computer Engineering, Politecnico di Milano, 2012.
	Master of Science in Computer Science, University of Illinois at Chicago, 2012.
PUBBLICATIONS:	X. Bao, D. Dragomir-Daescu, R. Entwistle, A. Gnemmi, D. Marsala, D.P. Pau: “An automated method to estimate femoral shape and mineral mass.”, IASTED 2012.